SEA6

Strategic Environmental Assessment of the Irish Sea

The distribution and extent of methane-derived authigenic carbonate

A.G. Judd

March 2005

Department of Trade and Industry

DTI Strategic Environmental Assessment, Area 6 (SEA6)

The distribution and extent of methane-derived authigenic carbonate

A.G. Judd

This report was produced as part of the UK Department of Trade and Industry's offshore energy Strategic Environmental Assessment programme.

The SEA programme is funded and managed by the DTI and coordinated on their behalf by Geotek Ltd and Hartley Anderson Ltd.

EXECUTIVE SUMMARY

There are no published reports of methane-derived authigenic carbonate (MDAC) in the SEA6 area, but carbon isotope data have confirmed that the cemented hard grounds of two areas studied for the SEA6 project, Texel 11, and Holden's Reef, are composed of MDAC. Geophysical surveys, sampling and photographic surveys of other parts of the SEA6 area have confirmed that indicators of gas seepage (seep plumes, and pockmarks) are present in several other areas, and that acoustic turbidity (shallow gas) is widespread.

Gas bubbles rising from large pockmarks, and high methane concentrations in sediment porewaters and the water column, suggest that MDAC is likely to be present in the pockmark areas of the north-western Irish Sea. However, detailed surveys failed to confirm that it is present, perhaps because of the softness of the seabed sediments. Geophysical survey data suggest that the conditions for MDAC formation are also present in Lune Deep and Wigtown Bay, however no sampling or photography were undertaken in these areas. In the Central Irish Sea evidence of seabed fluid flow and MDAC indicators were not identified; strong tidal currents and coarse, mobile sediments are not conducive to the preservation of such features on the seabed.

Remarkable features of three sites studied in this area (Harvey Trench, Texel 10, and Texel 11) are substantial seabed cliffs in which sediments of late-Pleistocene age are exposed having been truncated by erosion. These cliffs, and the substantial rocky reef, Pisces Reef, may be worthy of further investigation. Considerable erosion (> 80 m in Harvey Trench) has occurred in a relatively short period of geological time. Although the tidal currents may be responsible for this erosion, evidence of extensive shallow gas, and (in Texel 11) widespread MDAC formation lends support to the speculation that erosion has been assisted by gas venting.

Potential sources of both microbial and thermogenic methane are present beneath much of the SEA6 area. The widespread presence of potential methane sources, shallow gas, indicators of seabed fluid flow suggest that MDAC is not restricted to Texel 11 and Holden's Reefs. MDAC 'risk' assessment suggests that MDAC is widely distributed in the SEA6 area, from offshore Pembrokeshire to the Firth of Clyde; most occurrences are likely to be of limited extent and associated with faults or outcrops of coarse sediment layers that permit gas migration from sub-cropping source rocks. Nevertheless, the two new occurrences of MDAC, Texel 11 and Holden's Reefs, reported here are extensive. Mapping showed that Holden's Reefs cover an area of about 40,000 m^2. MDAC reefs are distributed over areas totalling >500,000 m^2 in the Texel 11 survey area; this includes a continuous reef (a 6 to 8-m high cliff) >500 m long. No comparable sites have been reported hitherto on the UK continental shelf, and several questions regarding their formation remain to be investigated.

1. INTRODUCTION

Methane-derived authigenic carbonate (MDAC) is formed as a consequence of the anaerobic oxidation of methane by consortia of microbes. The structures are composed of the normal seabed sediment bound by a carbonate (principally $CaCO_3$) cement; the carbon of this carbonate is derived from methane (CH_4). Therefore, a fundamental requirement for the formation of these structures is the presence of methane. MDAC formation occurs close to the boundary between oxic and anoxic sediments where sulphate (SO_4) derived from seawater is fully utilised (by sulphate-reducing bacteria), and anaerobic methane-generating microbes exist. This '*sulphate-methane transition zone*' (SMTZ) generally lies within a few metres of the seabed. The processes leading to MDAC formation are adequately described in the literature, and it is not necessary to provide details here (for a summary see Judd, 2001).

The distribution of these features in UK waters in poorly known. Although sometimes regarded (e.g. Johnston, *et al.*, 2002) as being confined to pockmarks (seabed depressions formed by the escape of fluids through soft, fine-grained sediments), it is known that natural gas seeps are not confined to pockmarks, and occurrences of these carbonates in sediments not suitable for pockmark formation are known in the North Sea and elsewhere.

Whilst it is difficult to detect MDAC remotely, it is possible to identify sites at which it is likely to occur by identifying 'shallow gas', (gas in the sediments close to the seabed), gas seeps, and seabed features associated with gas seepage (pockmarks, mud volcanoes etc.); methane is the most common gas in marine sediments. At present there are no published reports of MDAC in the UK sector of the Irish Sea, although evidence suggesting its presence on mounds in the Irish sector was presented by Croker, Garcia-Gil *et al.* (2002). However, there are reports of widespread shallow gas, some pockmarks, and a few seeps.

The main purpose of this report is to summarise the available information relevant to MDAC in the SEA6 area, including data acquired as part of the SEA6 survey programme during 2004, and to evaluate the likely distribution and extent of MDAC in the SEA6 area. As the presence of methane in seabed sediments is an essential prerequisite for MDAC formation, this report first considers the distribution of sources of methane, and migration pathways which might permit deep-sourced methane to rise to the seabed sediments. Areas with a high potential for MDAC formation are then considered, using evidence from the literature and from the SEA6 surveys.

The Irish Sea was subject to a pilot study (*The Irish Sea Pilot*; Vincent *et al.*, 2004) as part of the development of a UK strategy for marine nature conservation. The *Irish Sea Pilot* considered 'Marine Landscapes', 'nationally-important marine features', and 'nationally-important marine biodiversity areas'.

The Irish Sea Pilot survey programme produced data relevant to the following:

Marine Landscapes:
- Aphotic reefs
- (Irish) Sea Mounds
- Gas structures

Nationally-important marine features:
- Deep sponge communities
- Deep-water mud basins

Nationally-important marine biodiversity areas:
- Cold seeps, Muddy Hollow, Tremadog Bay
- Lune Deep, Morecambe Bay
- Irish Sea cold seeps
- Pingo, north-west of Anglesey
- Irish Sea Mounds, north-western Irish Sea.

1.1 Relevant literature

Relevant studies of the sediments of the Irish Sea include academic studies undertaken by the University of Wales (both Aberystwyth and Bangor), and regional surveys, maps, and report work by the British Geological Survey (BGS). It must be emphasised that most of the relevant work was undertaken during the 1960s, 1970s, and the early 1980s since when the technology for data acquisition, processing, and presentation has advanced considerably, as discussed in detail by Tappin, 2004); scientific ideas also have progressed. Consequently there is a need to re-evaluate old data and to acquire new data in order to satisfy the needs of SEA6.

1.1.1 BGS publications

The maps (*Anglesey*: James and Wingfield, 1990, Wingfield, 1990; *Cardigan Bay*: James and Wingfield, 1988, Wingfield, *et al.*, 1990; *Clyde*: Evans, 1985; *Isle of Man*: Wingfield, 1985; *Lake District*: Wingfield, 1983; *Liverpool Bay*: Wingfield, 1984) and regional reports (*Irish Sea*: Jackson, *et al.*, 1995; *Cardigan Bay and the Bristol Channel*: Tappin, *et al.*, 1994) published by the British Geological Survey provide the most up-to-date syntheses of the geology of the SEA6 area. These publications provide the context in which other literature is considered. Specifically, these publications have been used to evaluate the distribution of conditions conducive to methane formation and its migration towards the seabed.

1.1.2 Holden’s Reef

Investigations by the Countryside Council for Wales (CCW) described a carbonate reef, Holden’s Reef, in Cardigan Bay as a submarine structure made by leaking gas. The results of CCW’s initial investigations provided essential information for studies of Holden’s Reef (described in Section 3.6.2 of this report). The CCW investigations, described by Pelagial (2005), are on-going.

1.2 SEA6 Survey Data

A specific objective of the SEA6 surveys was to investigate possible occurrences of MDAC in examples of a range of the geological contexts present in the SEA6 area. To that end 12 study areas were identified, as shown in Figure 1. Two surveys were undertaken during the period 24th August to 31st October 2004:
- geophysical surveys (S/V *Meridian*): single-beam echo sounder (SBES), multi-beam echo sounder (MBES), side-scan sonar (SSS), and chirp sub-bottom profiler (SBP);
- photography, seabed sediment sampling, and water sampling (S/V *Kommandor Jack*).

Details of the equipment used are presented in Appendix I.

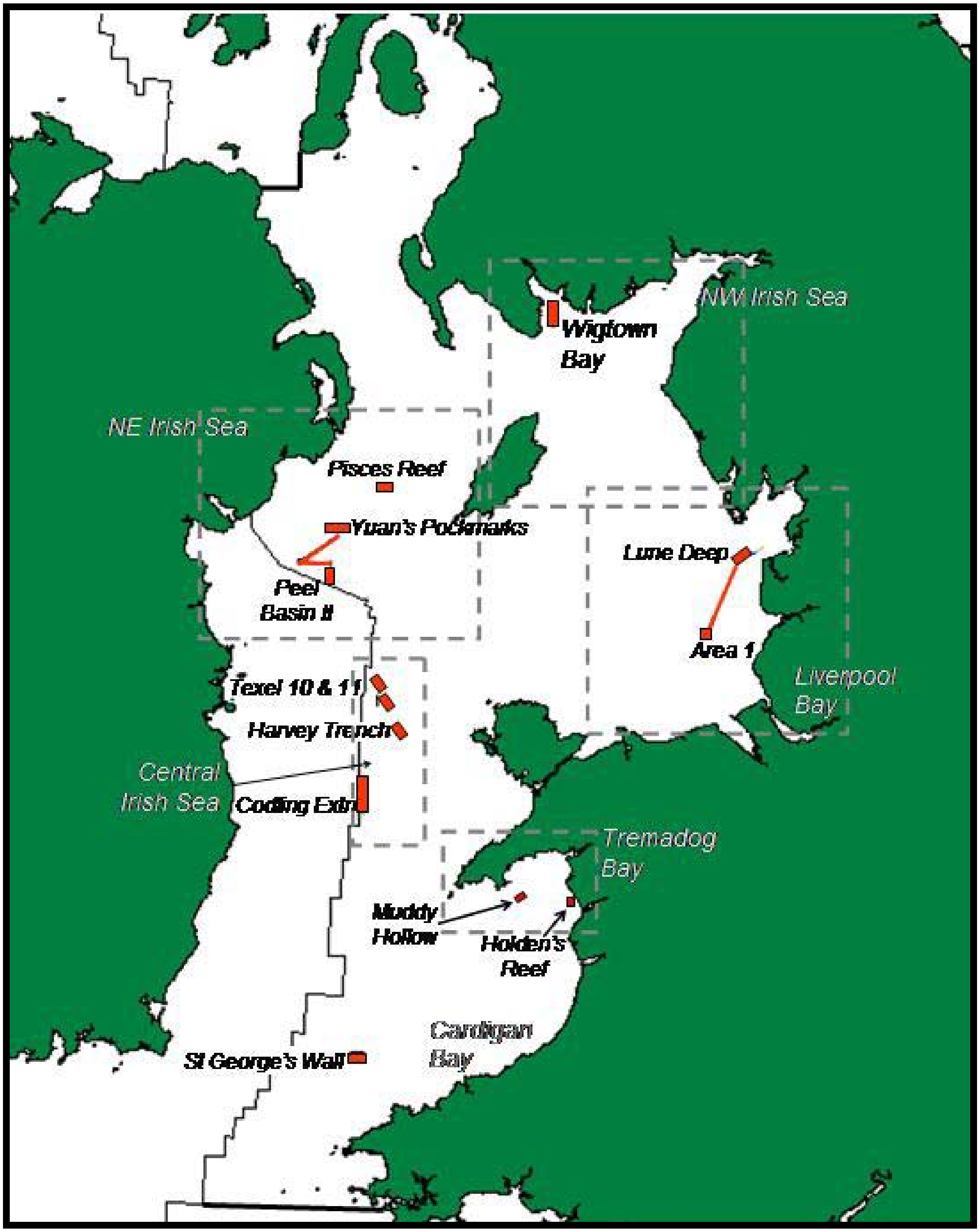

Figure 1: Study areas visited during the 2004 SEA6 surveys.

The geophysical surveys were undertaken in areas selected on the basis of a literature review; the photographic and sampling surveys were focussed primarily on areas that appeared, from preliminary interpretations of the geophysical data, to be most favourable for the formation of MDAC. The surveys were time-limited and affected by operational factors (including poor weather conditions), consequently they were restricted to the areas discussed below. These areas were selected as examples of the various geological contexts present in the Irish Sea in which MDAC may be present.

Geophysical, sampling, and photographic surveys of Tremadog Bay also undertaken as part of the SEA6 operation (using SV *Lia*) are reported separately (Osiris Projects, 2005), but details relevant to this study are included in this report.

1.2.1 Sample analyses

Samples collected during the second (*Kommandor Jack*) survey and the Tremadog Bay (*Lia*) survey were subjected to analyses as follows:

Sediment porewater methane concentration

Sub-samples of grab samples were preserved for subsequent analysis by gas chromatography at the University of Newcastle upon Tyne according to the following method (modified from Abrill *et al*., 2002):

A 1.5 to 2.0 ml plug of sediment was collected using a sawn-off syringe and placed in pre-weighed 14 mL serum bottles with 2.5 ml miliQ water and 0.5 ml of 10 mM $HgCl_2$; the headspace was then flushed with nitrogen before the bottle was sealed with a rubber cap. Samples were shaken briefly to mix $HgCl_2$ with Milli-Q and porewater in order to arrest further microbial activity and stored until analysis in the dark at room temperature. Analysis was performed within 2 weeks of sample collection. The serum bottles were shaken vigorously for 10 minutes in order to allow equilibration of the methane dissolved in the porewater-MilliQ-$HgCl_2$ mixture with the Nitrogen headspace. A 2 mL aliquot of the equilibrated headspace was then removed from the serum bottles by displacement with MilliQ into a gas tight syringe. The gas sample was then injected into gas chromatograph (Shimadzu GC-8A) with a flame ionisation detector (FID). Chromatographic separation was performed on a 2m, 1/8" packed column with Porapak-Q as the packing material under isothermal conditions (60°C) and nitrogen carrier gas. The instrument was calibrated daily using primary gravimetric standards (BOC gases Ltd.). The serum bottles were then re-weighed, dried overnight at 60°C and re-weighed again in order to derive the weight of sediment added, porosity and volume of porewater for each sediment sample plug. Methane solubility was calculated according to the Bunsen solubility given the n-situ salinity and temperature of the water overlying the sediment cores and normalised to the volume of porewater in each sample. Methane concentrations are expressed as normal to porewater or per cent saturation with respect to atmospheric equilibrium.

Results are presented in Appendix II.

Scanning Electron Microscopy examination of carbonate samples

Samples of carbonate collected during grab sampling operations were subjected to analysis by scanning electron microscope (SEM) at the Advanced Chemical and Materials Analysis (ACMA) laboratory in the University of Newcastle upon Tyne. The low vacuum SEM used (an FEI XL30 ESEM-FEG) permits detailed imaging of samples that have not been coated in carbon or gold. Integral thin-window energy-dispersive X-ray analysis (EDX) permitted light element analyses to be performed on selected individual sample grains.

Carbon and oxygen isotope analyses

Sub-samples of carbonate collected during grab sampling operations were subjected to carbon and oxygen isotope analysis by Iso-Analytical Ltd.

Aliquots of fine sample powder were placed in clean glass septum-capped vials. The vials were then sealed and the headspaces flushed with pure helium (99.995%). After flushing, ~0.5 ml of pure phosphoric acid (prepared according to the procedure of Coplen *et al.*, 1983) was injected into the vials and mixed with the sample powder to convert available carbonate material to CO_2. As the samples were treated as calcites, the reaction temperature of the acids on the sample material was performed at room temperature (~23°C) for a period of 24 hours. Any dolomite present in the samples would not have converted to CO_2 as this requires a 95°C reaction temperature for 3 hours. Standard reference materials were prepared in the same manner as the samples, as were some previously-analysed MDAC samples included with the batch as an additional control.

The CO_2 gas was then analysed by continuous flow isotope ratio mass spectrometry. In brief, the CO_2 was flushed from the septum vial using a double holed needle and resolved on a packed column gas chromatograph. The CO_2 then entered the ion source of a Europa Scientific 20-20 IRMS and was ionised and accelerated. Here, gas species of different mass were separated in a magnetic field, then simultaneously measured using a Faraday cup collector array at m/z 44, 45 and 46.

The reference material used for these analyses was a laboratory $CaCO_3$ standard IA-R022 ($\delta^{13}C_{v\text{-}PDB}$ -28.63‰ and $\delta^{18}O_{v\text{-}PDB}$ -22.69‰), which is traceable to NBS-19 Limestone which is distributed as an isotope reference standard by the International Atomic Energy Agency, Vienna. During analysis, NBS-19 limestone ($\delta^{13}C_{v\text{-}PDB}$ +1.95‰ and $\delta^{18}O_{v\text{-}PDB}$ -2.2‰), NBS-18 calcite ($\delta^{13}C_{v\text{-}PDB}$ -5.00‰ and $\delta^{18}O_{v\text{-}PDB}$ -23.00‰), IAEA-CO-8 carbonatite ($\delta^{13}C_{v\text{-}PDB}$ -5.80‰ and $\delta^{18}O_{v\text{-}PDB}$ -22.7‰), and IA-R022 were analysed as quality control check samples.

Results are presented in Appendix III.

Water methane concentration

Water samples were preserved for subsequent analysis by gas chromatography at the University of Newcastle upon Tyne according to the following method:

Samples were collected in 1 litre glass volumetric flasks with a length of silicone tubing directly from the water sampler. The tube was inserted into the bottom of the flask and allowed to oveflow, avoiding the formation of bubbles. 0.5 ml of 10 mM $HgCl_2$ were added in order to arrest further microbial activity and a glass stopper was inserted to store headspace-free samples. The samples were stored in the dark at room temperature until analysis. Sample analysis was performed according to Upstill-Goddard et al. (1996). Briefly, a known volume of compressed air headspace with known methane concentration was created with an automated manifold and the sample equilibrated by sparging for 10 minutes. The headspace was then used to flush a 1 mL sample loop and the latter injected into a gas chromatograph (Shimadzu GC-14B) equipped with an FID. Chromatographic separation was performed on a 2m, 1/8" packed column with Porapak-Q as the packing material under isothermal conditions (60°C) and nitrogen carrier gas. The instrument was calibrated daily using primary gravimetric standards (BOC gases Ltd.). Methane solubility was calculated according to the Bunsen solubility given the in-situ salinity and temperature of the water samples. Methane concentrations are expressed as normal to porewater or per cent saturation with respect to atmospheric equilibrium.

Results are presented in Appendix IV.

2 METHANE FORMATION AND MIGRATION

Methane is formed in continental shelf sediments such as those of the Irish Sea by two processes: microbial methane is formed by the degradation of organic matter in sediments from the seabed to a depth of about one kilometre; thermogenic methane (along with other hydrocarbons) is formed at greater depth by the thermocatalytic breakdown on residual organic matter.

Within the SEA6 area potential sources of thermogenic have been identified in rocks of Permian to Cretaceous age; there is potential for microbial methanogenesis in Tertiary lignites and Holocene muds. As can be seen from Figs. 2a and b, this suggests that there is at least a potential for methane to be present over the majority of the SEA6 area. Several publications (Pantin, 1977; Jones, *et al.*, 1986; Yuan, *et al.*, 1992) reported that indicators of shallow gas are confined to areas of muddy sediment, and therefore suggested that the gas was probably generated within these sediments by microbial activity. However, although extensive in muddy sediments, acoustic turbidity (an indicator of gas) is not present throughout the muddy areas. Croker, 1995) argued that there is also evidence of shallow gas in areas characterised by coarse-grained Quaternary sediments, and favoured a deeper, thermogenic source, probably in the Carboniferous.

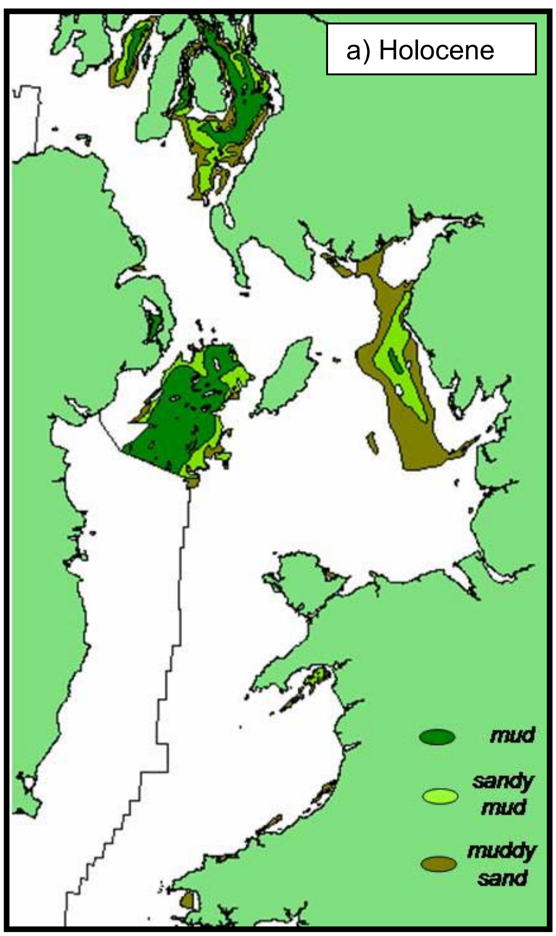

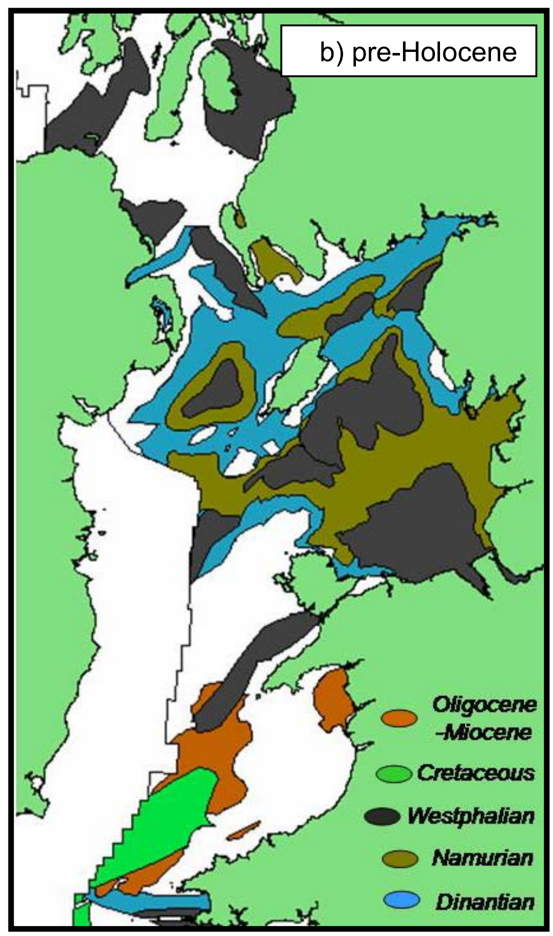

Figure 2: Potential sources of methane: a) Holocene; b) pre-Holocene
[from data compiled by L.H. Tizzard].

The most significant pathways enabling gas to migrate towards the seabed are:

- Inclined permeable strata: where such strata are exposed at the seabed or sub-crop beneath surficial sediments, as they do in the areas indicated on Fig. 3, seabed fluid flow is possible.
- Faults: in the Irish sector of the Irish Sea fluid migration has been strongly associated with the Codling Fault, and site survey reports from Liverpool Bay suggest that faulting may permit fluids to migrate into near-seabed horizons.
- Gas chimneys.
- Faulting and gas chimneys associated with salt diapirism: although salt is present in the Eastern Irish Sea Basin, the only significant salt migration structures are reported to be associated with the St George's Fault (west of Strumble Head, Pembrokeshire).

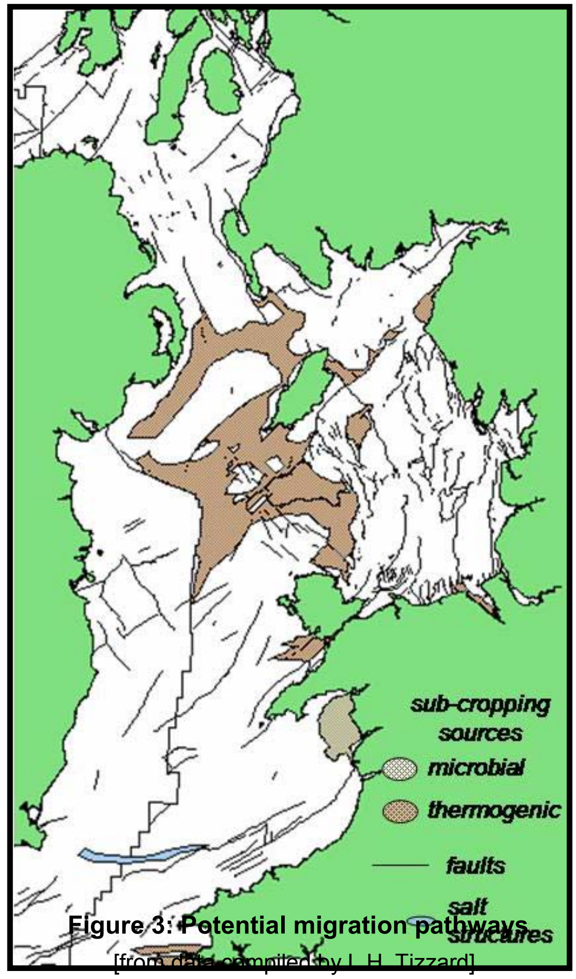

Figure 3: Potential migration pathways
[from data compiled by I. H. Tizzard]

In the absence of geological focusing, methane diffusing upwards is likely to be utilised beneath the seabed, at or beneath the SMTZ. Whilst this may result in the formation of MDAC, it is less likely that this MDAC will be exposed at the seabed unless some (natural or anthropogenic) erosion or disturbance exposes it. However, where focussed seabed fluid flow exceeds the rate of utilisation the SMTZ may rise to the seabed enabling MDAC formation at or very close to it.

3 EVIDENCE OF METHANE-DERIVED AUTHIGENIC CARBONATE

Methane-derived authigenic carbonate (MDAC) is formed where methane is present in seabed sediments. Identifying shallow gas, seeps, and other features associated with seabed fluid flow are easier than identifying MDAC; mapping them is useful preliminary stage in 'MDAC-hunting'.

The first published discussion of shallow gas in the Irish Sea was by Pantin (1977) who reported the presence of acoustic turbidity on shallow seismic reflection (pinger) profiles from various parts of the Irish Sea. He interpreted them as shallow gas. He noted that, in places, the gas seemed to be trapped beneath impermeable layers to produce a flat top to the acoustic turbidity. He reported that in other instances the gas seemed to have been trapped by more than one layer, producing stepping of the 'gas front' (the top of the acoustic turbidity). Geophysical evidence of shallow gas was also identified by Caston (1966), Al-Shaikh (1970), Caston (1966), Jones, *et al.*, (1986), Taylor Smith (1987), Hession and Whittington (1987), and Hession (1988); acoustic turbidity is also visible on seismic profiles published by Garrard, 1977), although it was not identified as such in the publication. The BGS maps and reports summarise these shallow gas occurrences (with a few omissions) and others identified during the BGS mapping programme; they are included on Fig. 4.

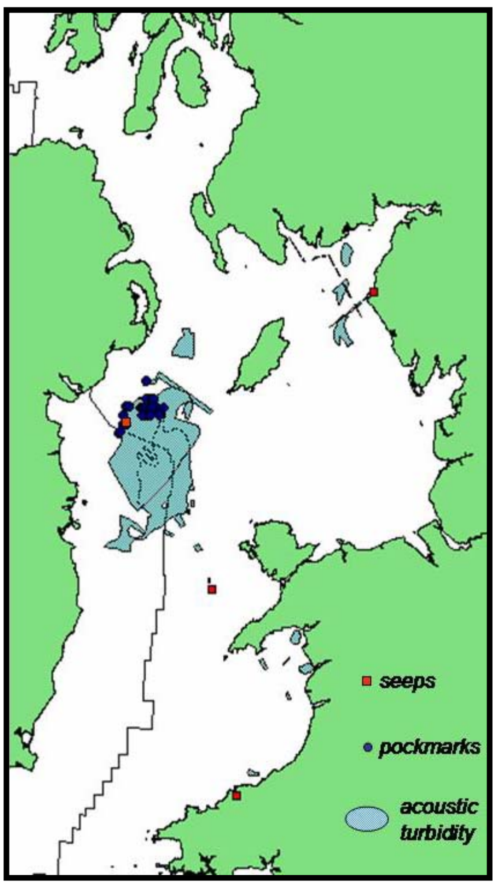

The BGS Regional Reports (*Cardigan Bay and the Bristol Channel* and *Irish Sea*) suggest that there are no seabed features formed by fluid escape apart from some pockmarks and seabed domes in the gassy areas of the Western Mud Belt. Gas seeps are identified in two places on the *Anglesey* Quaternary Geology map (see Fig. 4); the evidence supporting these identifications is not mention. Relevant research not summarised in the BGS publications includes work by Yuan (Yuan, 1994; Yuan, *et al.*, 1992) on the gassy sediments of the Western Mud Belt, and various contributions from Croker (Croker, 1994, 1995; Croker, Garcia-Gil, *et al.*, 2002; Croker, Monteys, *et al.*, 2002). The latter are based on cable route surveys (undertaken between 1986 and 1992) and various research cruises (1995-2002).

Figure 4: Indicators of seabed fluid flow [from data compiled by L.H. Tizzard]

The areas from which evidence of seabed fluid flow have been reported are discussed in the following sections.

3.1 Liverpool Bay

Although there are no specific published reports of seabed fluid flow in Liverpool Bay, the presence of extensive Carboniferous source rocks (see Fig. 2b) and petroleum accumulations (some of which are being exploited commercially), and the extensive fault network (illustrated in Fig. 3) suggest that seabed fluid flow is likely. Also, a BGS seismic across Lune Deep indicated the presence of shallow gas (Wingfield, 1984), and water column targets (sometimes indicative of gas seeps) are prolific on BGS shallow seismic (pinger) profiles of part of Liverpool Bay. To investigate these possibilities geophysical surveys were undertaken in two geologically distinct areas in Liverpool Bay (see Fig. 5).

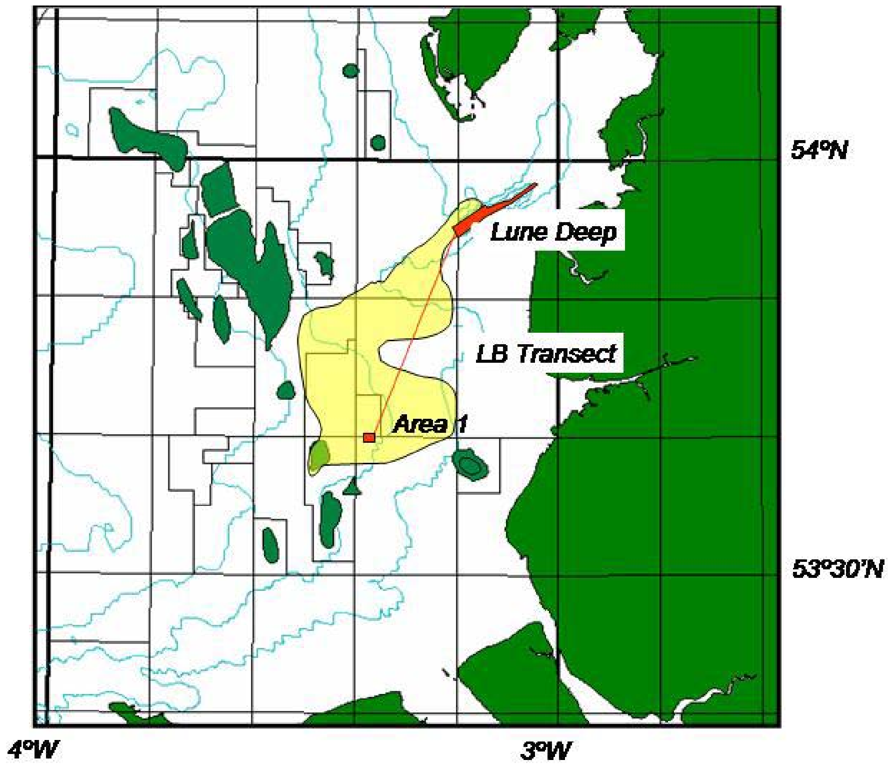

Figure 5: Survey operations in Liverpool Bay. Survey areas (Lune Deep and Area 1) are shown in red; the Liverpool Bay transect is indicated by the red line. Oil and gas fields are shown in dark green; bathymetric contours are at 10 m intervals; the yellow ornament indicates the area in which acoustic water column targets were recorded on BGS Pinger data.

3.1.1 Lune Deep

Lune Deep is an enclosed bathymetric deep at the mouth of Morecambe Bay. Acoustic turbidity (interpreted as shallow gas) is present in the sediments on the south-eastern side of the deep according to Wingfield (1984). The SEA6 survey area covered the entire deep water area, and extended inland towards the north-east (Fig. 6).

Figure 6: Lune Deep: MBES bathymetry. The cross section, A-B (inset), of one of the two deep areas shows the steepness of the seabed slope (<17º) between the exposed rock (north-west side) and the sediment infill of the 'Deep'. The locations of Figs. 7 (profile C-D) and 8 are indicated.

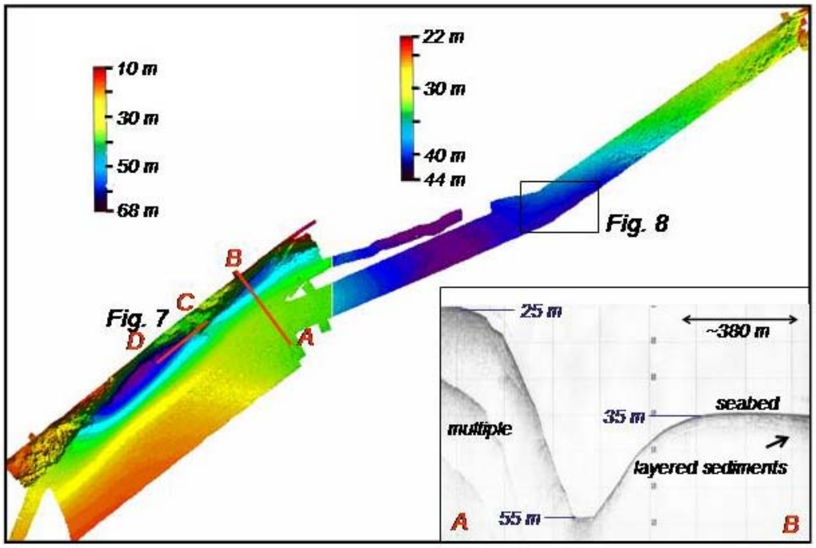

The northern edge of the deep is constrained by exposed rock; hollows seem to have a thin fill of softer sediment. In deeper water the sediments are of variable character; some are relatively coarse-grained, others are fine-grained and well-layered. Interpretation of sub-seabed reflections is complicated by the similarity between hard reflectors (rock) and acoustic turbidity. In some places the outcropping rock outcrops are clearly seen extending beneath the seabed sediments, but in others evidence of gas (acoustic turbidity) was identified (see Fig. 7).

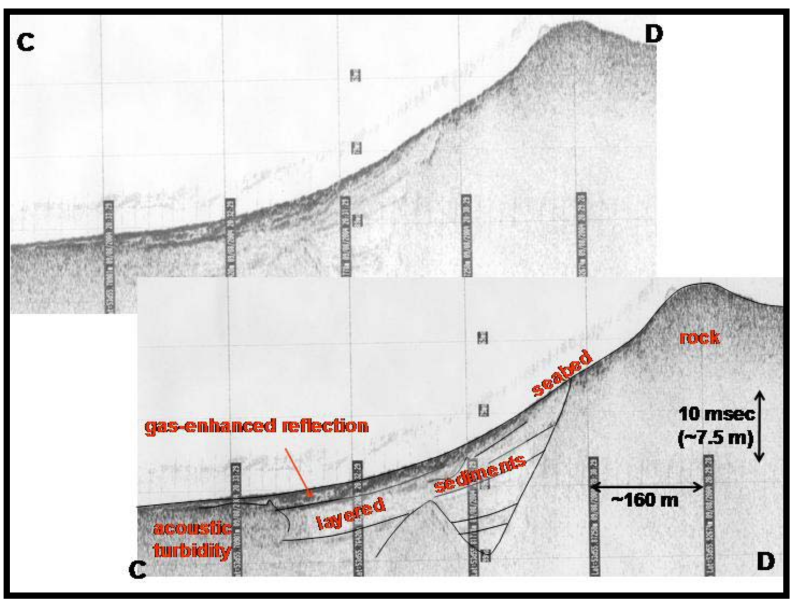

Figure 7: Seismic (chirp) profile C-D (interpretation bottom right) showing the similarity between the acoustic reflections presented by rock and acoustic turbidity (shallow gas). [The location is marked on Fig. 6.]

In places where the seabed sediments are coarse (minor sand waves are visible on the MBES data) gas might be able to migrate through the seabed without leaving visible evidence. However, pockmarks (evidence of seabed fluid flow) are present where the sediments are finer grained (see Fig. 8).

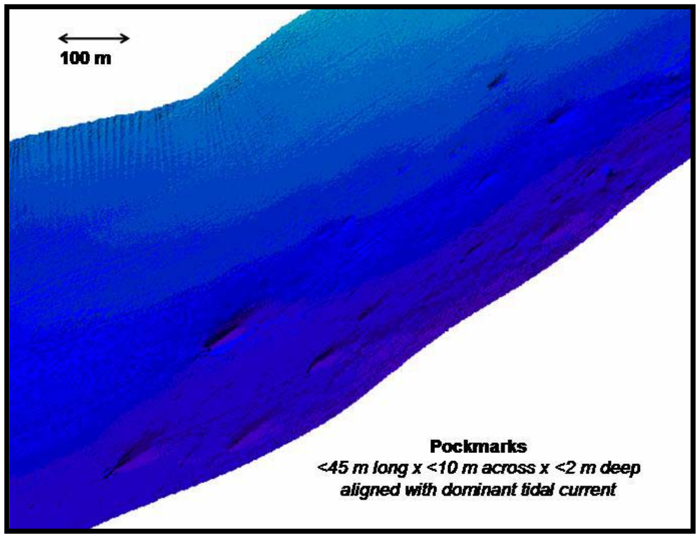

Figure 8: MBES bathymetry showing pockmarks [The location is marked on Fig. 6.]

Together, the occurrence of acoustic turbidity (shallow gas) and pockmarks (evidence of seabed fluid flow) suggest that active methane seepage, and therefore MDAC, is likely in this survey area. However, operational matters prevented photography and sampling, so no conclusive evidence is available.

3.1.2 Area 1

In Liverpool Bay, gas from Carboniferous source rocks may evade entrapment within Triassic reservoirs by migrating along faults. 'Area 1', located between the Asland gas field and the Lennox oil field and crossed by a north-south fault, was identified as having possible gas seepage on the basis of previous site survey data. However, on the SEA6 survey no evidence was found of gas at, or close beneath, the seabed. Side-scan sonar data revealed many trawl scars, but no evidence of seabed features indicative of seepage.

3.1.2 Liverpool Bay transect

A transect across Liverpool Bay between Area 1 and Lune Deep was undertaken in order to investigate dense acoustic water column targets (?gas or fish) identified on BGS Pinger data (project 72/07) within a large area off the Lancashire coast (see Fig. 5). Water column targets were seen in areas comparable to those of 1972. However, the nature of the targets suggests that they are fish, and there is no evidence of gas within the seabed sediments. This may be a function of the sediment type; gravelly muddy sand and gravelly sand according to the BGS sediment map. Such sediments are likely to be permeable, so any gas may not regularly pass through specific pathways. Analyses of the methane concentration of the seawater in this area may shed light on the nature of the water column targets, but water sampling was not possible during the SEA6 surveys.

3.2 North-Eastern Irish Sea

Much of the north-east Irish Sea is underlain by potential methane sources of Carboniferous and/or Holocene age, as can be seen from Figure 2. Large areas of acoustic turbidity (shallow gas), first reported by Pantin (1977), are indicated to the north and east of the *Isle of Man* by the BGS Regional Report (Irish Sea; Jackson *et al.*, 1995) and maps (*Liverpool Bay*, *Lake District*, and *Isle of Man* sheets; Wingfield, 1983, 1984, and 1985), as indicated in Fig. 4. Although Jackson *et al.* (1995) implied that shallow gas is confined to three areas within the Eastern Belt of the Western Irish Sea Formation, Wingfield's cross-sections indicate that gas is more widespread, some apparently lying beneath sandy sediments. Interpreted seismic sections suggest that in most cases the gas lies in Quaternary pro-glacial lagoon clays, as seen in Fig. 9.

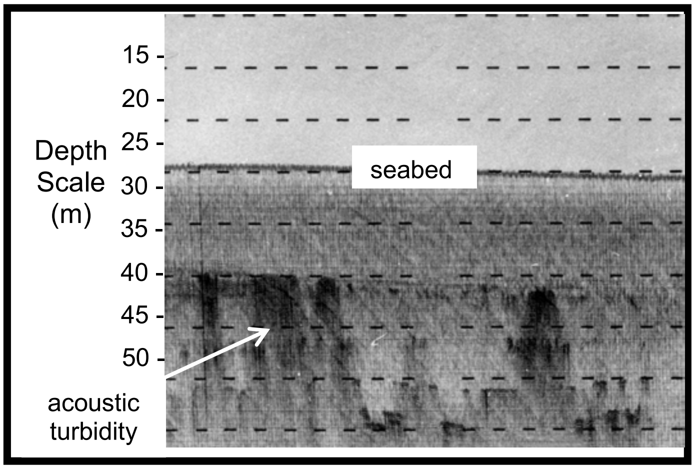

Figure 9: Acoustic turbidity (shallow gas) in the north-eastern Irish Sea. [Image courtesy of H.M. Pantin]

Two of the areas identified by Jackson et al were partially covered by another SEA6 survey (Cruise A; see Figure 10), but the only recorded indications of seabed fluid flow were a few pockmarks (see Fig. 11).

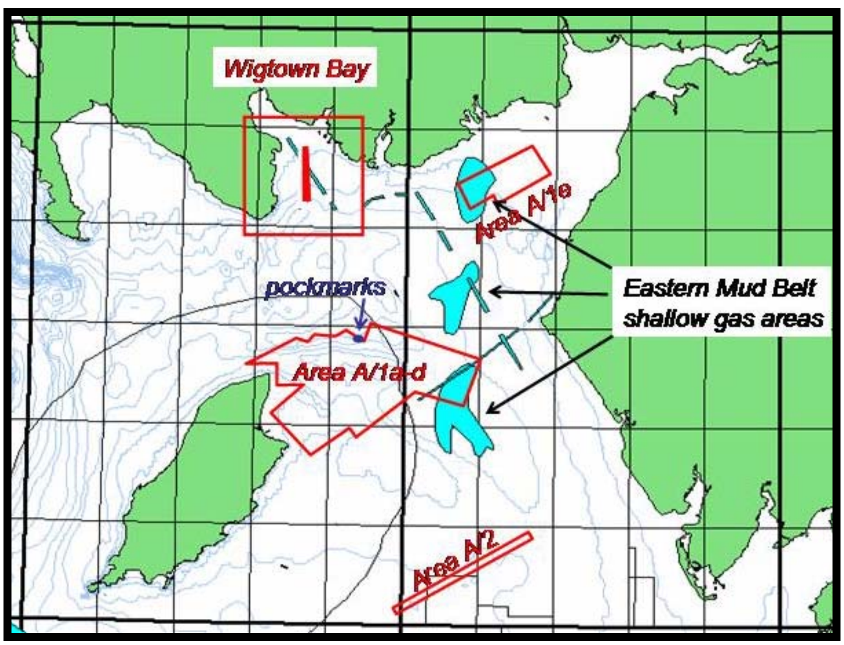

Figure 10: North-East Irish Sea. Shallow gas areas identified in BGS publications are shown in light blue. SEA6 Cruise A areas 1a-d, 1e, and 2 are outlined in red; a small area in which pockmarks are apparent on Cruise A MBES data is indicated in dark blue. The Wigtown Bay survey area, Fig. 12, is outlined red.

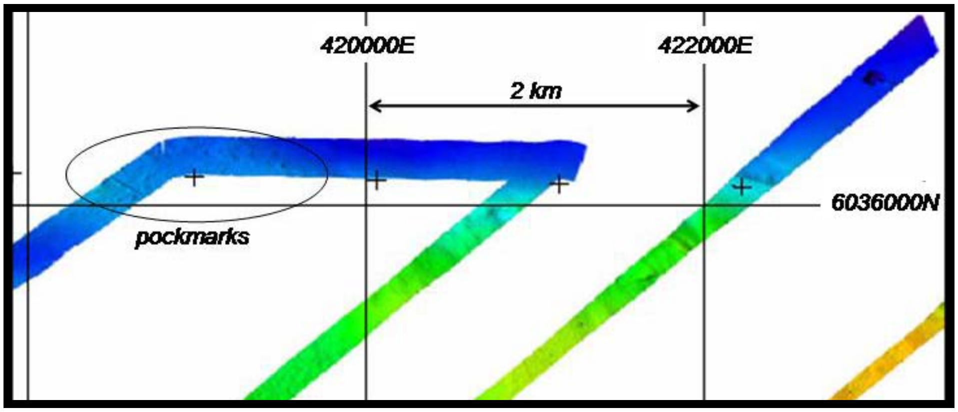

Figure 11: Pockmarks on Cruise A MBES data. The location is indicated on Fig. 10.

Although there is potential for the presence of MDAC in these areas, for logistical reasons surveying was restricted to part of Wigtown Bay.

3.2.1 Wigtown Bay

The Wigtown Bay survey area was designed to cover the BGS cross-section indicating shallow gas (see Figs. 10 and 12).

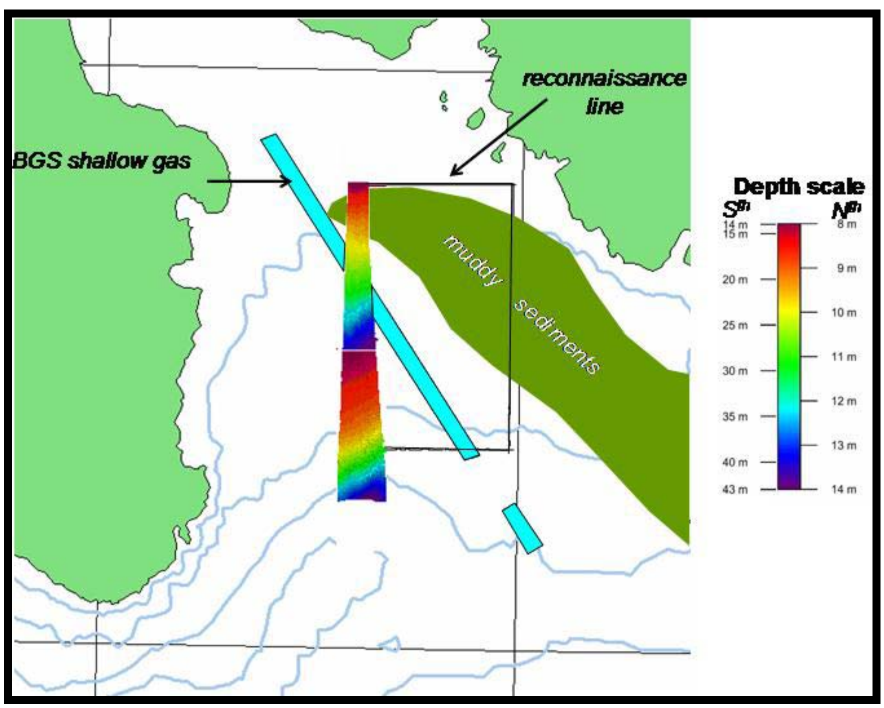

Figure 12: Wigtown Bay survey area showing MBES bathymetry. Weather and sea conditions permitted no coverage of the area with muddy sediments (muds, sandy muds, and muddy sands) other than the reconnaissance lines indicated.

Chirp profiles (e.g. Fig. 13) showed that acoustic turbidity and gas-enhanced reflections are extensive; water column targets (WTCs), some of them very intense, are plentiful. No seabed features associated with seabed fluid flow were identified on the side-scan sonar data; however, relatively coarse seabed sediment militates against focussed fluid flow, so features such as pockmarks are unlikely to form. Conditions did not permit survey work to extend into the area of muddy sediments where focussed flow is more likely.

Two areas in which seismic evidence suggests gas rising to within <2 m of the seabed were identified. Such locations may be suitable for the formation of MDAC, however time constraints permitted neither photography, nor sampling in this area, so it is unknown whether or not MDAC is present.

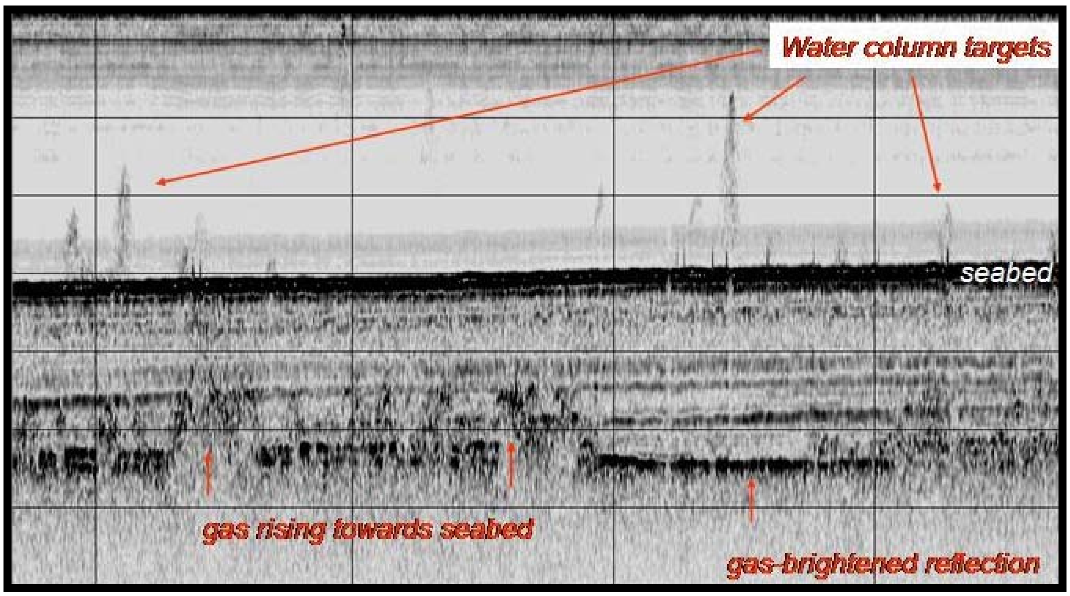

Figure 13: Wigtown Bay sub-bottom profiler (chirp) data example showing evidence of gas beneath the seabed and water column targets (gas seeps or fish). Timing lines are at 2 ms (approximately 2 m) intervals.

3.3 North-Western Irish Sea

The majority of the north-western Irish Sea is also underlain by potential methane source rocks of Carboniferous age (Fig. 2b) which, in places, sub-crop beneath the surficial sediments (Fig. 3). The widespread occurrence of acoustic turbidity in the Western Mud Belt (Fig. 14) has led various authors to suggest that the gas is microbial, sourced from the late-Quaternary sediments. It is found mainly where these muddy sediments are at least 36 m thick. Yuan (1994) found total organic carbon (TOC) to vary between 1.3 and 5.2% within the areas of acoustically turbid sediments, and between 1.2 and 3.7% outside these areas, suggesting that methanogenesis might be possible within the seabed sediments both inside and outside the areas with acoustic turbidity. However, the smell of H_2S, which may be indicative of anaerobic methane oxidation, was not confined to cores from these areas. In fact the extent of this acoustic turbidity is uncertain as various authors have indicated different boundaries. Two well-defined large areas, the larger being about 1,500 km^2 and the smaller about 110 km^2 in area have been identified (see Fig. 14), but acoustic turbidity also occurs in a few small pockets between these areas. Yuan (1994) noted that the area of gassy sediments extended to where the sediments are sandier; this is further south than indicated on the *Anglesey* Quaternary sheet (Wingfield, 1990).

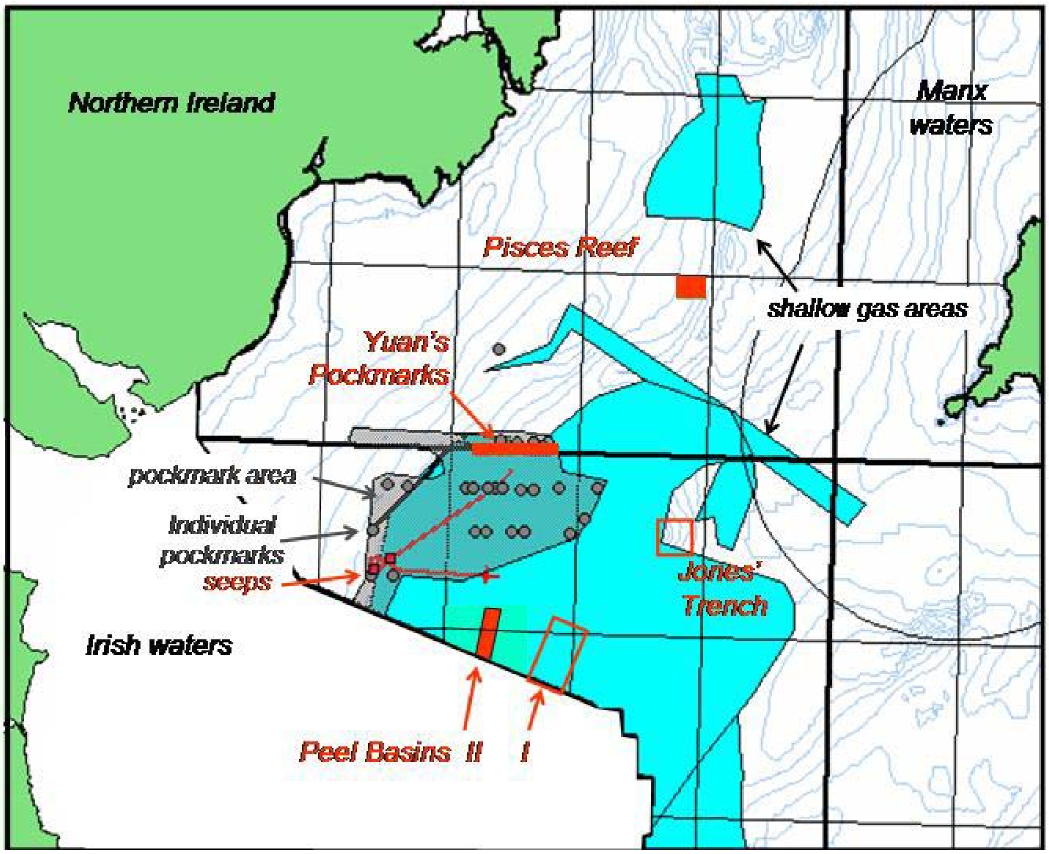

Figure 14: North-West Irish Sea. Shallow gas areas (light blue) as mapped by several authors; pockmark areas in grey, individual pockmarks (grey spots) mapped by Yuan (1994); seeps (red spots) indicated by Wingfield (1990). Peel Basin I and Jones Trench are areas surveyed by Croker (PAD, Ireland); Pisces Reef, Yuan's Pockmarks and Peel Basin II are SEA6 survey areas; the red line indicates the transect between Yuan's Pockmarks and Peel Basin II.

The conclusion that the acoustic turbidity represents gas is supported by the occurrence of gas bubbles in several cores described by Jones *et al.* (1986) and Yuan (1994); Jones *et al.* presented analyses demonstrating the presence of methane (>0.2 $nM.l^{-1}$). Gassy sediments were encountered at sub-seabed depths down to 36 m in BGS borehole 89/15.

Yuan (1994) noted that the depth of the top of the acoustic turbidity (the 'gas front') generally lies at a depth of 4 to 8 m below seabed, but deepens to 14 to 20 m towards the edges of the gassy area. Yuan found that where the proportion of coarse (silt and sand) particles increases there is a tendency for 'plumes' or 'pillars' of acoustic turbidity (also reported by Jones et al, 1986) to extend towards the seabed; however, Croker (1994) related these plumes to topographic highs in underlying bedrock (Fig. 15).

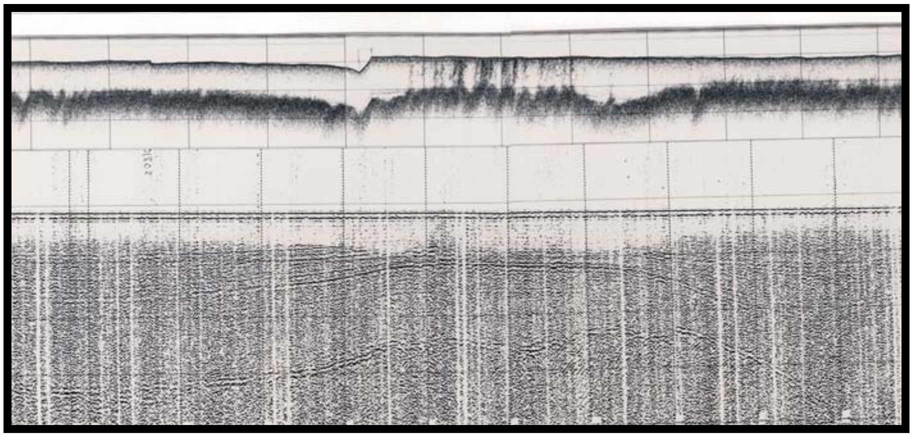

Figure 15: Acoustic turbidity rising beneath seabed in soft sediments in the Western Mud Belt, Irish Sector. The gas plumes (upper, pinger, profile) are located above a topographic high seen on the lower, sparker, profile (from Croker 1994).

Some plumes underlie seabed domes (e.g. Fig. 16a), indeed all the seabed domes recorded were underlain by gas plumes. Most domes are a few hundred metres across and <1 m high. In many cases (e.g. Fig. 16b) gas plumes are not associated with seabed doming.

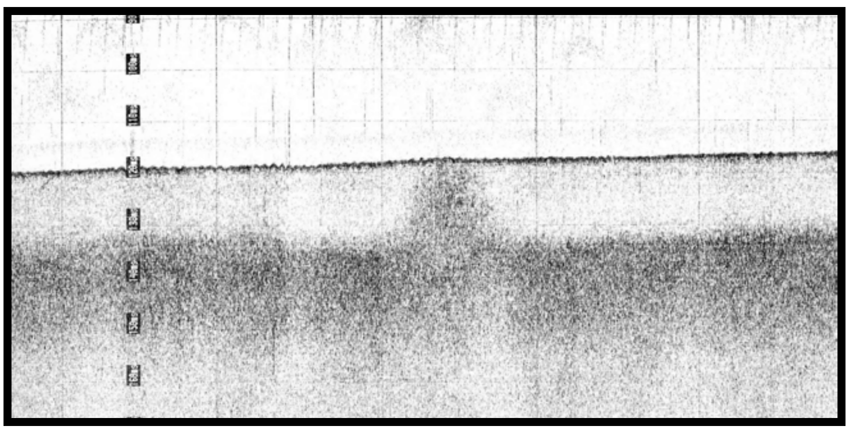

Figure 16a: Plumes of acoustic turbidity rising beneath seabed domes in the Western Mud Belt.

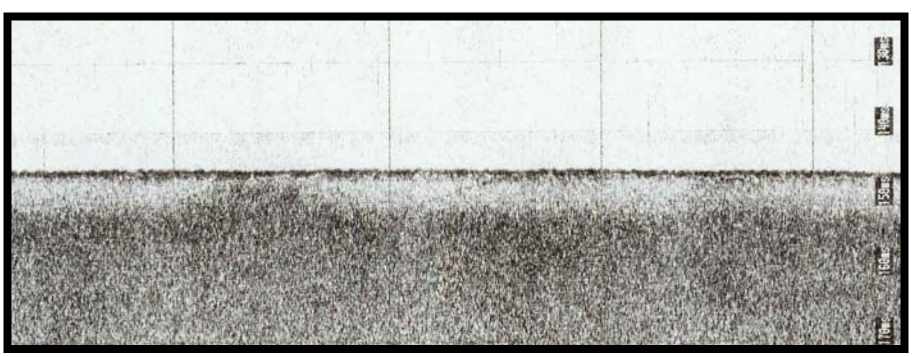

Figure 16b: Plumes of acoustic turbidity rising to a flat seabed in the Western Mud Belt.

Pockmarks seem to be few in number when compared to pockmark areas in the North Sea (see Judd, 2001); Yuan reported <40 individuals (although as pockmarks were not visible on his side-scan sonar records, the number may have been under estimated). They are limited to areas with water depths of 50 to 100 m. Most lie within the area of gassy sediments, but a few lie outside it. Most are between 70 and 110 metres in diameter, and less than 1.5 m in depth. However, Yuan estimated the largest (located close to 53º55.06'N 5º28.61'W) to be about 400 m across and 6 m deep.

Water column turbidity, representing particles in the water, observed on echo sounder images presented by Yuan (1994), appears to be significantly higher where the seabed sediments are gassy. The greatest concentrations occur over seabed trenches within gassy areas, where the gas front is closer to the seabed, and where gas plumes rise to the seabed. Yuan was unable to comment on whether this turbidity was associated with the gassy sediments, or with the location of the 'Western Front', a hydrological boundary between stratified and well-mixed water masses.

The above review indicates the widespread nature of shallow gas in the north-western Irish Sea; the pockmarks and seeps indicate seabed fluid flow. More recent work (Croker, 1998) in the Peel Basin I and II and Jones' Trench areas (indicated on Fig. 14) has supported the general conclusions of the earlier workers (Jones and Yuan). These conclusions suggest that MDAC is likely to be present in this area. Additional surveys to locate MDAC for SEA6 targeted specific areas (indicated on Fig. 14).

3.3.1 Pisces Reef

Reports from a 1972 BGS (then IGS) submarine (*Pisces*) dive described rocky outcrops (a potential carbonate mound?) located between the main areas of acoustic turbidity marked on Fig. 14 (Eden *et al.*, 1973). The geophysical data demonstrated that this is a substantial rocky outcrop lying within an area of soft muddy sediments. Visual inspection confirmed that it comprises exposed bedrock and rocky boulders (Fig. 17), with soft sediments infilling hollows and gullies. Magnetometer data indicate that the bedrock is probably of igneous origin (P. Croker, personal communication, 2005). The soft sediments are similar in appearance to those of the deeper water surrounding the reef; by the density of burrows, both are inhabited by *Nephrops* (Fig. 18).

This 'reef' is extensive; it is 600 m wide, >1.4 km long, and stands about 60 m above the normal seabed (Fig. 19).

Figure 17. Rocky boulders at the foot of Pisces Reef.

Figure 18. *Nephrops* and burrows in soft sediment infilling the central gully on Pisces Reef.

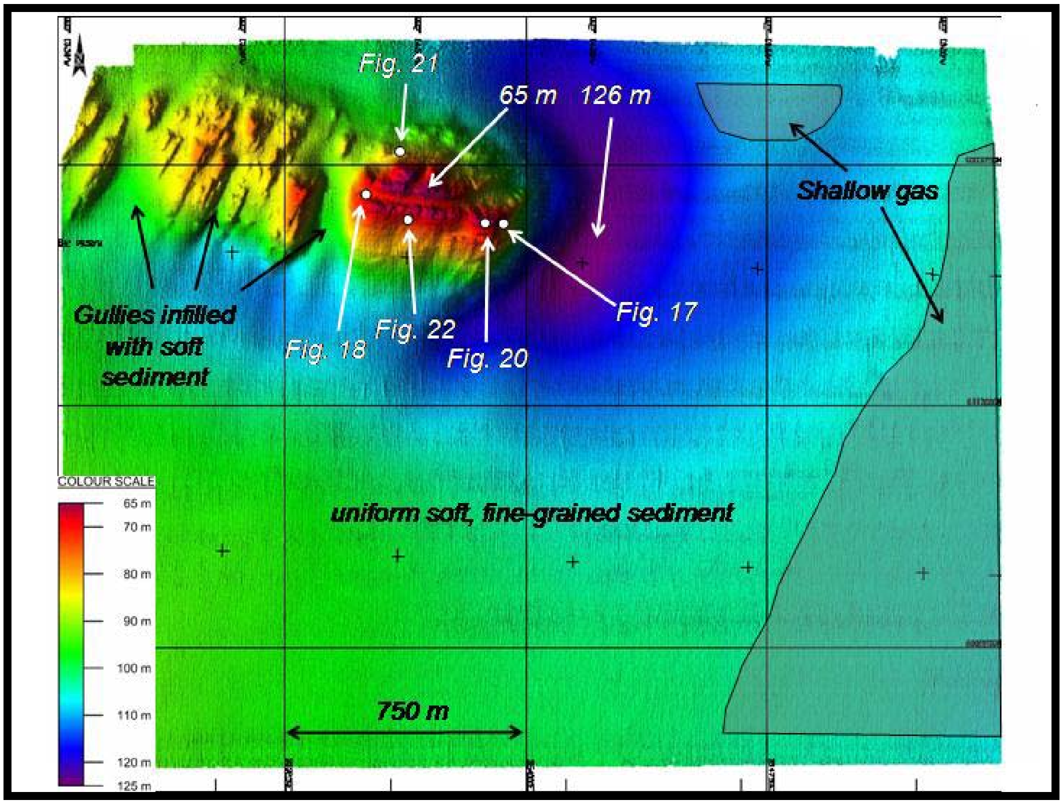

Figure 19: Pisces Reef. Multi-beam echo sounder image of the bathymetry. The extent of acoustic turbidity (shallow gas) and sediment-filled gullies are indicated, as are the locations of the photographs shown in Figures 17, 18, 20, 21 and 22.

Fig. 20. Epifaunal growth on boulders of Pisces Reef.

The rocky seabed supports a relatively dense epifauna (Fig. 20), and the density of water column targets was found to be significantly higher around and over the reef than elsewhere in this area. Photographs show that these are caused by shrimp and fish; the reef seems to be inhabited by large numbers of juveniles (Fig. 21 and 22).

Figures 21 and 22: abundant shrimp and juvenile fish around Pisces Reef.

Seismic profiles, side-scan sonar, and video evidence show that, beyond the reef, the seabed sediments are uniformly soft and fine-grained. They are cut by numerous trawl scars, but there are no pockmarks. Acoustic turbidity is present over parts of the east and south-east of the survey area; however this lies outwith the areas of acoustic turbidity mapped previously (Fig. 14). No indications of seabed fluid flow were identified.

3.3.2 Yuan's Pockmarks

A 9 km by 1 km survey area was selected in an area in which Yuan (1994) reported several pockmarks. The MBES image (Fig. 23) shows numerous small and three large pockmarks on an otherwise smooth seabed; the small (<20 m across) pockmarks are mainly in the deeper water towards the east of the area.

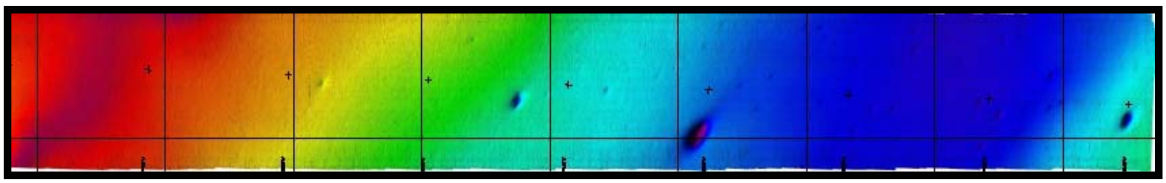

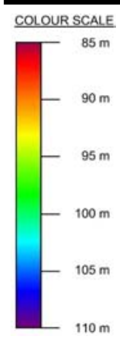

Figure 23: MBES bathymetric image of Yuan's Pockmarks area (grid lines are 1 km apart).

As in the area around Pisces Reef, the seabed sediments are very soft (too soft to support the weight of the camera frame) fine-grained muds; they are typical of the Western Mud Belt according to Jackson *et al*. (1995). The profiler records showed these sediments to be acoustically-transparent, and acoustic turbidity was present over the majority of the survey area (Fig. 24). In the eastern half of the area it is exclusively found within the muddy seabed sediments, generally at depths of 10 to 30 ms (7.5 to 25 m) beneath the seabed. Over the majority of the western half of the area it is confined beneath the first sub-seabed reflector (late-Devensian to Holocene proglacial lagoon clays, according to Wingfield, 1985), rising in a few places into the overlying marine muds, but being absent over ridges in the underlying sediments (Fig. 25).

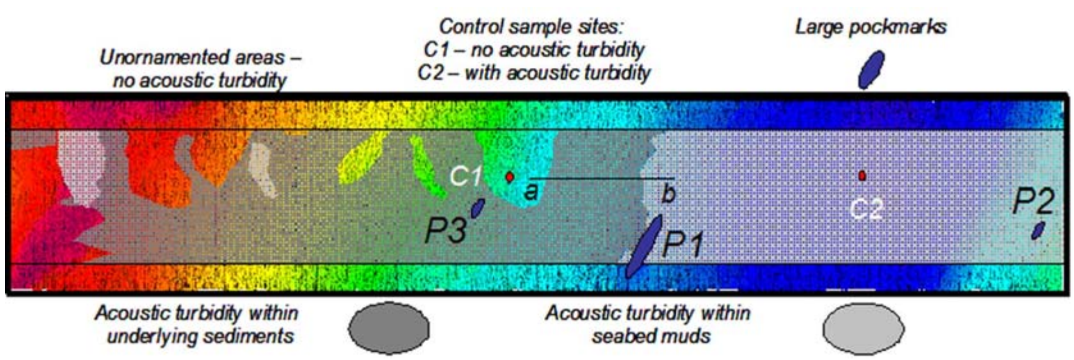

Figure 24: The extent of acoustic turbidity (shallow gas) in the Yuan's Pockmarks area. Note the location of seismic profile a-b.

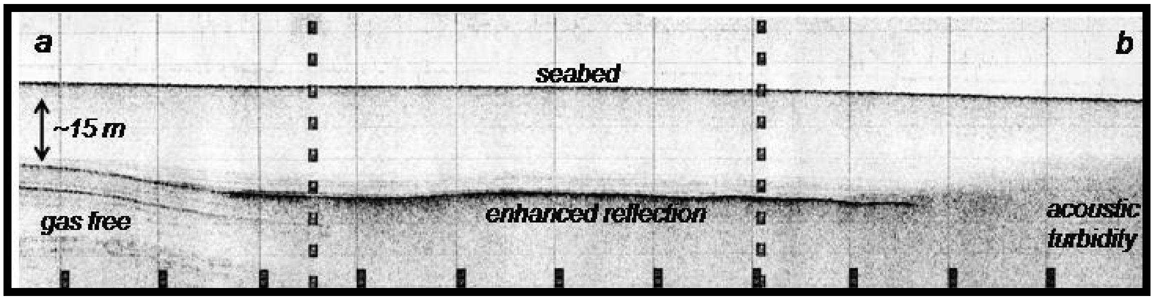

Figure 25: Seismic (chirp) profile a-b (location shown on Fig. 24).

The largest of the pockmarks (P1) is 250 m long by 150 m across with a maximum depth of 14 m below the surrounding seabed (117 m compared to 103 m). P2 and P3 are somewhat smaller: 210 m x 100 m x 6m, and 170 m x 90 m x 5 m respectively. Seismic profiles of P1 showed very strong seabed and near-seabed reflections, consistent with gas-enhanced reflections from sub-seabed sediment interfaces (Fig. 26); water column targets on the side-scan sonar are indicative of gas seepage (Fig. 27). Similar indicators at both P2 and P3 suggested that all three pockmarks are actively seeping gas; indeed gas bubbles were seen rising from the seabed inside pockmarks 1 and 3 (Fig. 28).

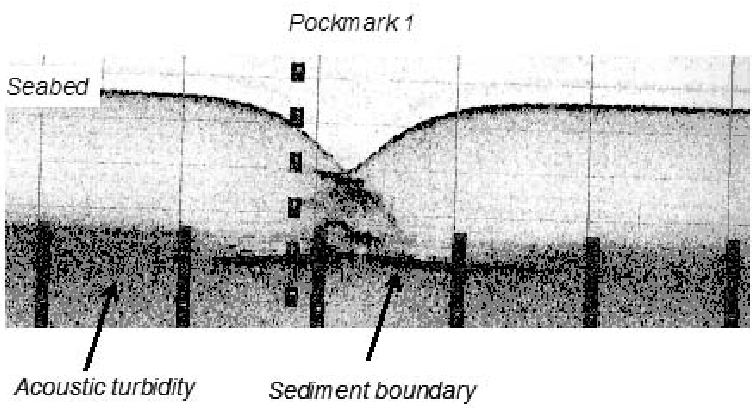

Figure 26: Seismic (chirp) profile across Pockmark 1. The sediment boundary beneath the pockmark is enhanced (brightened) by gas.

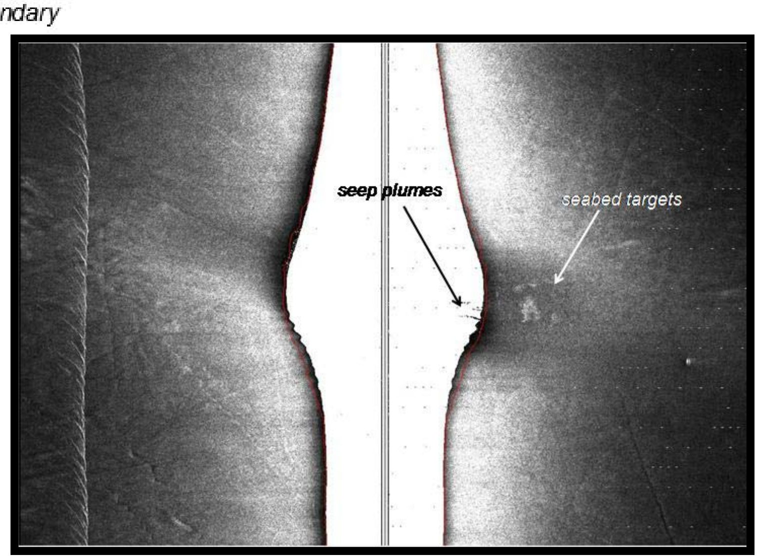

Figure 27: Side-scan sonar image showing a seabed target and gas seep plumes within Pockmark 1.

Figure 28. Gas bubbles rising from the seabed in Pockmark 1.

Detailed visual surveys of the three large pockmarks failed to identify any significant difference in the appearance of the seabed inside the pockmarks compared with outside them, or the control site. It is light grey in colour, and featureless apart from numerous burrows (Fig. 29). No evidence was seen of MDAC or features (black, sulphidic sediments or white mats of the sulphide-oxidising bacterium, *Beggiatoa*) normally associated with anaerobic methane oxidation, even at locations with distinct targets on the side-scan sonar (Fig. 27). Apart from *Nephrops* and other crustaceans, the benthic macrofauna seemed sparse, being limited to occasional starfish and anemones (Fig. 30).

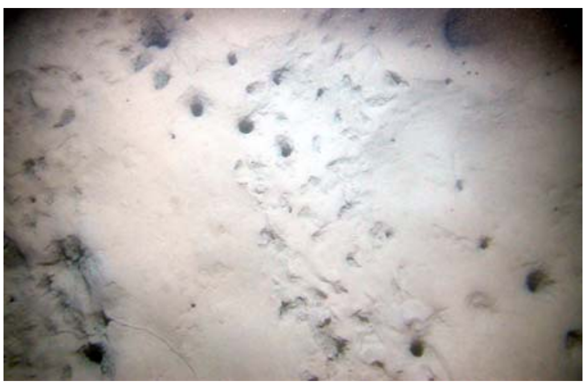

Figure 29. Seabed within pockmark 3; very soft sediment with abundant burrows.

Figure 30. Anemone (*Pachycerianthus multiplicatus*) and crustacean (prawn).

Methane concentrations in sediment porewaters proved to be significantly higher (4,700 and 4,200 nmol.l^{-1}) at two sites (the first in P3, the second within P1) than elsewhere; the degree of variability is seen in Fig. 31. Methane concentrations in the water column were measured in two profiles; one above Pockmark 1, the other at control station C2. At both sites concentrations in the near-bottom waters were very high, indicating a seabed source, and that the influence of this source continued to the sea surface (Fig. 32).

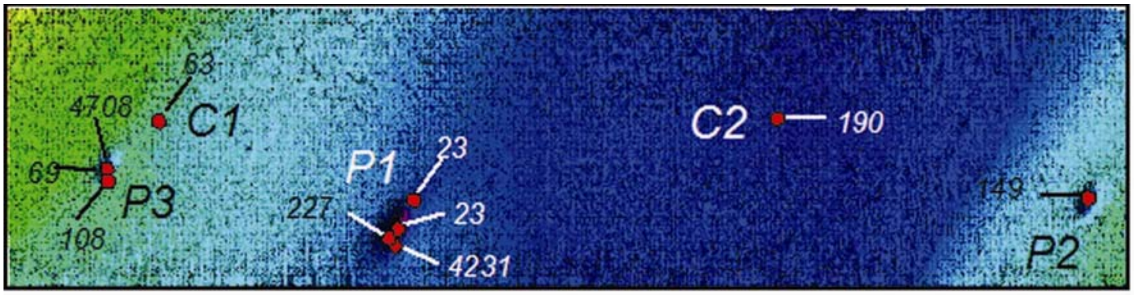

Figure 31: Methane concentrations (nmol.l^{-1}) in the porewaters of seabed sediment samples collected in Pockmarks 1, 2 and 3, and in at control sites: C1 over gas-free sediments, C2 over gassy sediments (see Fig. 24).

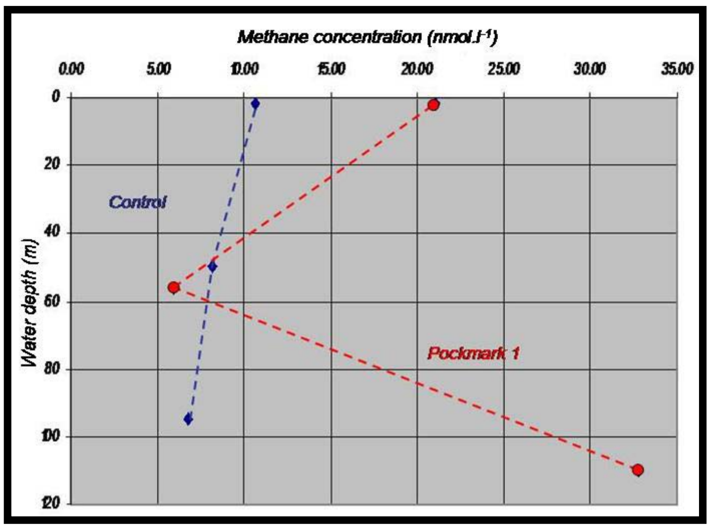

Figure 32: Water column methane profiles. The sea surface water concentrations represent 450 and 1375% saturation relative to the atmospheric concentration above the control and pockmark sites respectively. This indicates that the seawater at this site is a net source of atmospheric methane.

3.3.3 Peel Basin II

Reconnaissance surveys of two basins, Peel Basin I and II, conducted by PAD (Petroleum Affairs Division, Department of Transport, Energy and Communications, Republic of Ireland) identified during cable route surveys. Acoustic turbidity was found beneath much of Peel Basin I, and the whole of Peel Basin II. Detailed geophysical survey coverage of part of the UK portion of Peel Basin II was acquired for SEA6. This showed that there are two parallel elongate basins extending across the UK/Ireland median line (Fig. 33). The northern one is about 1 km wide by at least 5.5 km long, and about 35 m deeper than the surrounding seabed. Seismic profiles showed that acoustic turbidity not only covers almost the whole of the survey area (there are small areas in which it is absent), but also, the depth of the gas front (the top surface of the acoustic turbidity) consistently lies within the topmost sediment layer, except in a few places (see Fig. 34). In a few places it rises to within 2 ms of the seabed, and in a few it lies >20 ms beneath the seabed. There are no distinct sub-seabed gas plumes.

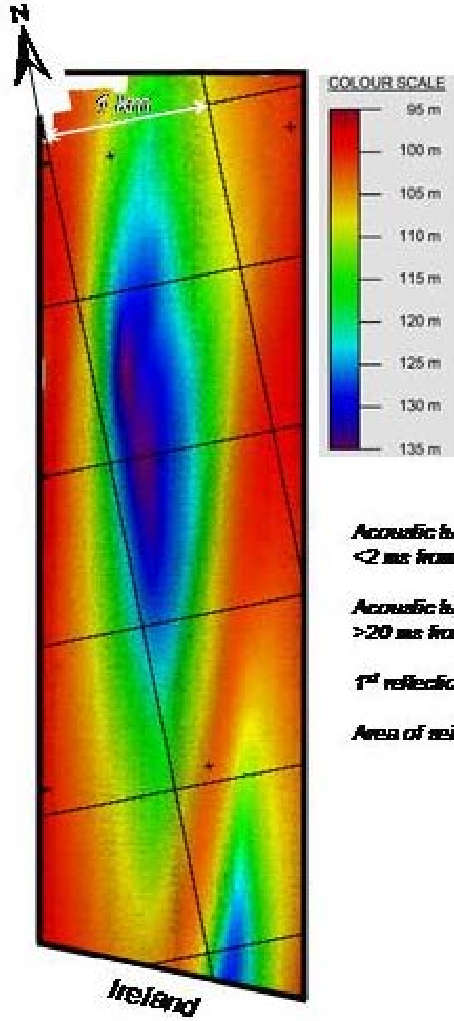

Figure 33: MBES bathymetry of the Peel Basin II survey area.

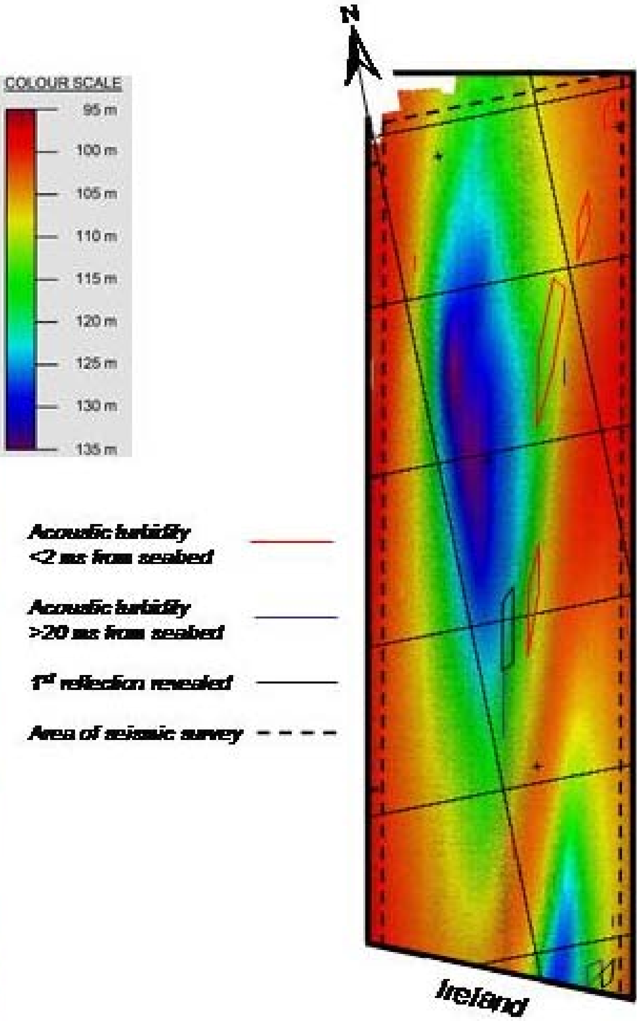

Figure 34: Distribution of shallow gas (acoustic turbidity); acoustic turbidity is present throughout the area covered by the seismic (chirp) survey, except where the first sub-seabed reflection is revealed. Variations in the depth of the gas front are indicated.

Bathymetry and side-scan sonar data showed that the seabed is uniformly smooth, with no topographic features (pockmarks or seabed domes), or variations in seabed reflectivity; that is, no variations in sediment type or evidence of MDAC. Despite the clear evidence of extensive shallow gas, it is concluded that microbial utilisation prevents gas rising to the seabed, and it is unlikely that MDAC is present at the seabed in this area; no photographs or samples were taken here.

3.4 Central Irish Sea

Cable route survey data used by Croker (1994, 1995) indicated the presence of shallow gas to the west of Anglesey; acoustic turbidity is also visible on sparker records from this area in the thesis of Al-Shaikh (1970). This gas is associated not with muddy seabed sediments, but with sandy sediments. Croker concluded that the gas is of thermogenic origin, probably derived from Westphalian Coal Measures or the Dinantian / Namurian Holywell Shale which subcrop beneath the Quaternary sediments. Croker (1994) argued that gas would be able to migrate easily through the Quaternary sediments (the Prograded Facies of the Western Irish Sea Formation), and suspected that substantial erosion by escaping gas was responsible for the formation of large trenches in the Central Irish Sea (Fig. 35). He presented data from three of these trenches (Harvey Trench, Central Trench, and Western Trench, the latter in Irish waters), showing evidence of gas close to the seabed, and in two cases (Central and Western Trenches) deep seismic data showing the juxtaposition of the trenches and sub-cropping inclined Carboniferous strata (Fig. 36). Prior to the SEA6 surveys, no data were available to assess whether or not MDAC is likely to be present in these trenches. Three areas were investigated during the SEA6 project.

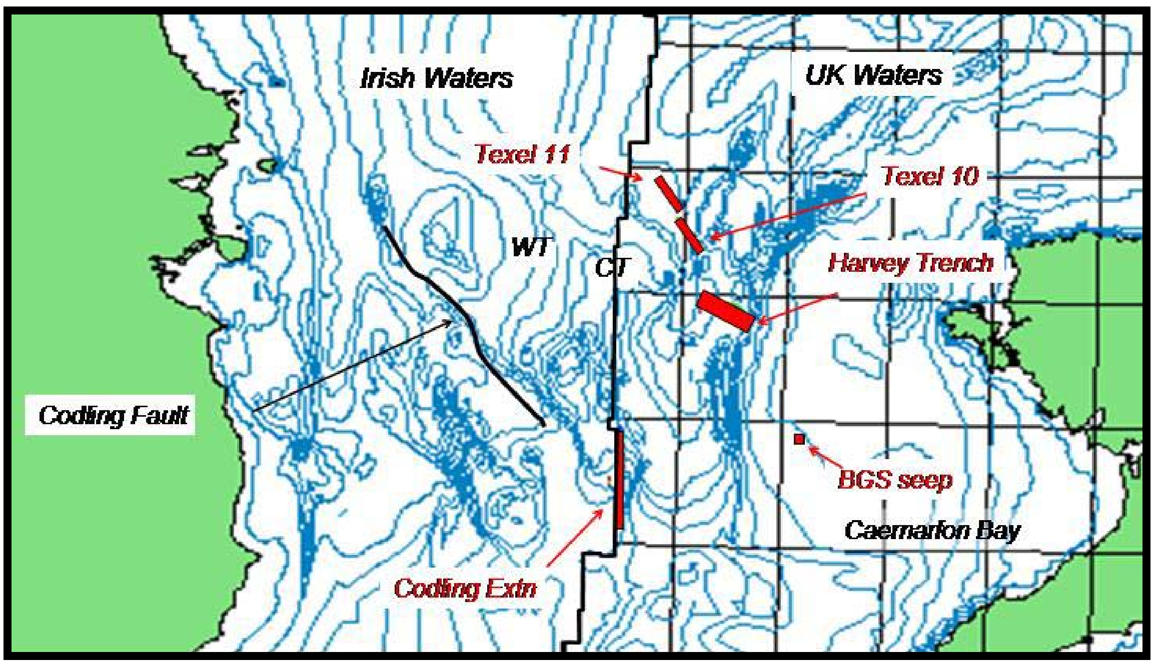

Figure 35: Central Irish Sea locations, the Codling Fault, and Caernarfon Bay. CT – Central Trench; WT – Western Trench.

3.4.1 Harvey Trench

Harvey Trench was originally described by Harvey (1966) during a study of large sand waves, and was subsequently described by Croker (1994). The trench is a major feature (3 km long, and 60 m deeper than the surrounding seabed) which overlies a major fault (Fig. 3). MBES bathymetry (Fig. 37) shows that the trench comprises two depressions, aligned approximately north-south, with a relatively flat plateau between. The 8 km long WNW-ESE SEA6 survey area effectively crosses five distinct areas: flat 'plateau' areas (water depth about 100 m) on either side of the site , and an isolated

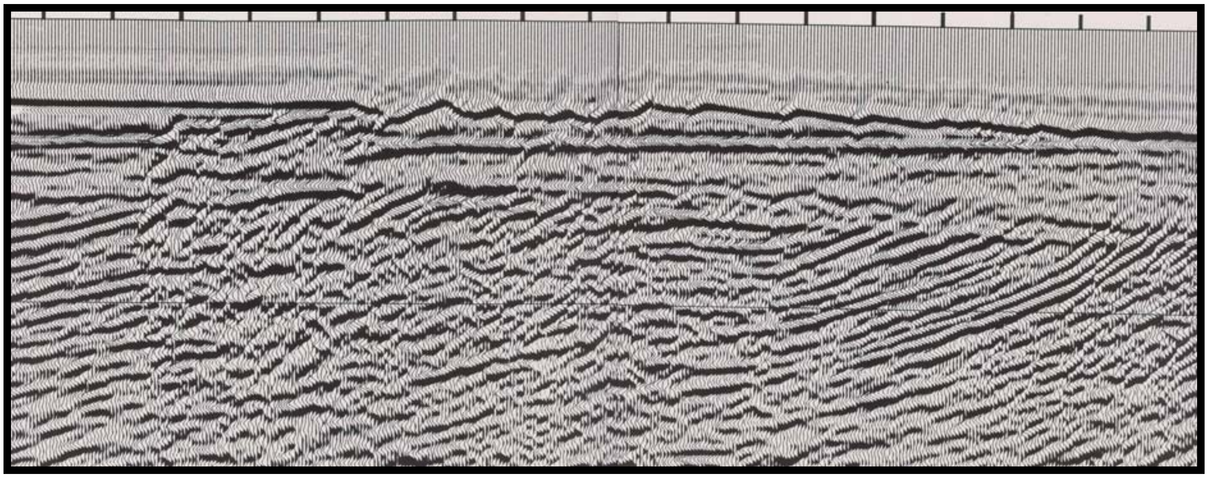

Figure 36: Air gun profile showing the coincidence between rough seabed topography (the Central Trench) and sub-cropping Carboniferous strata (from Croker 1994).

plateau area located between the two trenches. The western trench is about 1.7 km wide and 130 m deep, the eastern trench is about 3.6 km wide with a maximum recorded depth of 183 m, and the intervening plateau about 600 m wide.

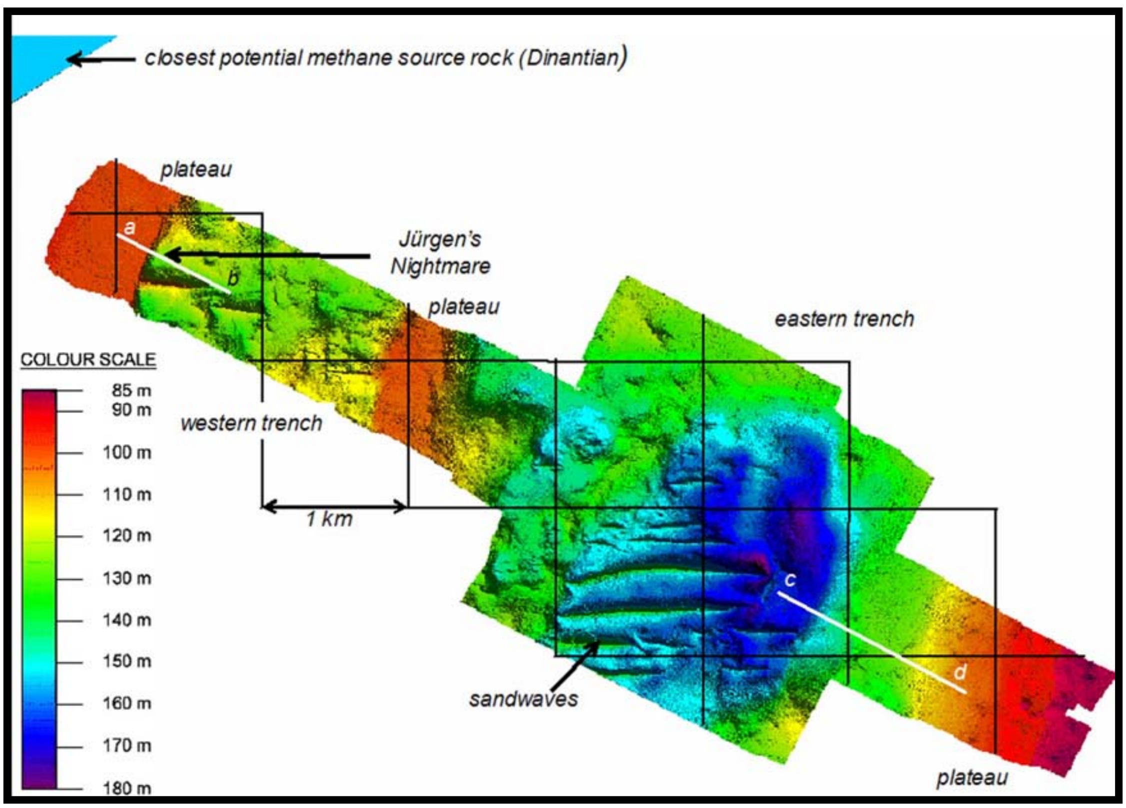

Figure 37: MBES bathymetry of Harvey Trench. The locations of seismic profiles a-b (Fig. 39) and c-d (Fig. 38) are indicated.

Seismic profiles (e.g. Fig. 38) show that the both the plateau areas and the trenches are underlain by gently dipping reflectors; these indicate sediments of the Prograded Facies of the Western Irish Sea Formation. This formation is described by Jackson *et al*. (1995) as comprising pro-deltaic and glaciomarine sediments deposited during ice-retreat in the Weichselian (the last glacial maximum of the late-Pleistocene). The layering indicated on the seismic sections suggests (relatively) fine-grained sediments with interbedded (relatively) coarse layers. They are clearly truncated in the sidewalls of the trenches which are evidently erosive features. The west sidewall of the western trench is particularly steep; at one point there is a vertical drop of 30 m over a distance of only 60 m (Fig. 39). This is referred to as *Jürgen's Nightmare*.

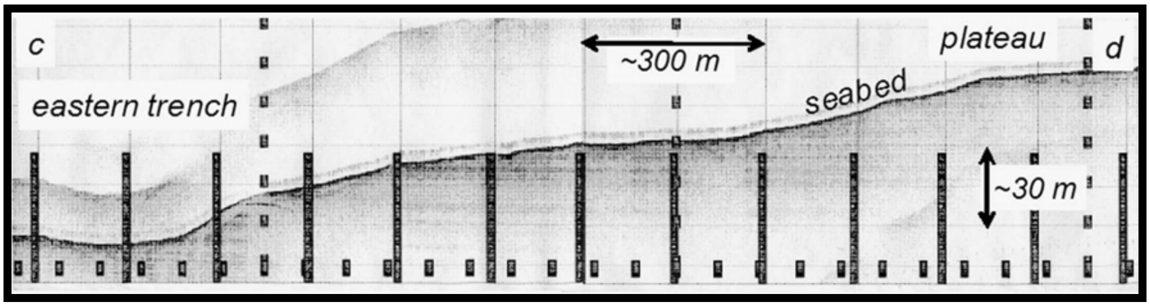

Figure 38: Seismic (chirp) profile from the plateau into the eastern trench. Layered sediments of the Prograded Facies are visible over much of this section, but in places they are obscured, possibly by shallow gas. The location is shown on Fig. 37.

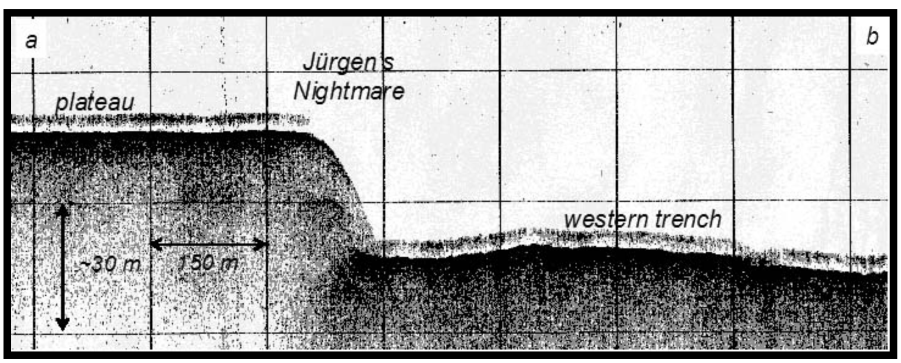

Figure 39: Seismic (chirp) profile from the plateau into the western trench, across Jürgen's Nightmare.

Sediment samples from the plateau were composed of stony/gravelly sand (Fig. 40). The steep cliff of *Jürgen's Nightmare* seems comparable to a scree slope. The 'scree' comprises pebbles, cobbles, and boulders, presumably derived from coarse layers in the Prograded Facies, sitting on a blue-grey clay (Fig. 41).

Figure 40: Coarse seabed sediments on the plateau above Jürgen's Nightmare.

Figure 41: Boulders lying on blue-grey clay of the Prograded Facies at the foot of Jürgen's Nightmare.

Figure 42: Clean, mobile sand on sandwaves in the eastern trench.

There are large sandwaves on the floor of the trenches (Fig. 37). The largest, in the eastern trench, are 1.4 km long, 120 m wide and 15 m tall; those of the western trench are 400 m long, 80 m wide and 10 m tall. The steepness of the sandwaves prevented the seismic system from resolving the peaks, representing them by indistinct dome-like features. Their near-symmetrical shape, and their east-west orientation is consistent with mobile bedforms affected by the strong north-south tidal currents, a significant feature of the Central Irish Sea. The strength of the tidal current proved challenging during the photographic survey as mobile sand (Fig. 42) impaired vision. Some seabed ridges run north-south (i.e. parallel to the dominant tidal currents and normal to the sandwaves). The deepest water in the trenches occurs in scour hollows at the ends of the sandwaves. Here the seabed is composed of cobbles and boulders in a coarse gravelly sand (Fig. 43). Away from the sandwaves, the seabed in the trenches is mainly covered by a coarse sediment with sand, pebbles and some shell accumulations; in some places it can be seen that these surficial sediments are underlain by clay (Fig. 44).

Figure 43: Boulder lying in the scour hollow at the end of a sandwave in the eastern trench; water depth >175 m.

Figure 44: Coarse surficial sediments lying on clay; western trench.

Within both trenches the sub-seabed reflections are generally obscured, either by signal starvation (i.e. the coarse seabed sediment is reflecting / scattering the sound energy) or by acoustic turbidity (i.e. the presence of gas). Distinguishing between the two is not a trivial task; although there are many clear instances of signal starvation, in other places the data interpretation is less clear. There are no clear indicators of reflection enhancement / brightening which would support the interpretation of shallow gas, nor are there any clear indications of seabed fluid flow. However, sediment porewaters from samples collected on the escarpment, on and at the base of Jürgen's Nightmare (Fig. 45), proved rich in methane (2,700 and 25,000 nmol.l^{-1}), contrasting markedly with the more normal concentration from a sample taken from the plateau (60 nmol.m^{-1}). This suggests that methane, perhaps from the Dinantian rocks further west, is migrating through the sediments of the Prograding Facies, to escape through the seabed on the face of the escarpment.

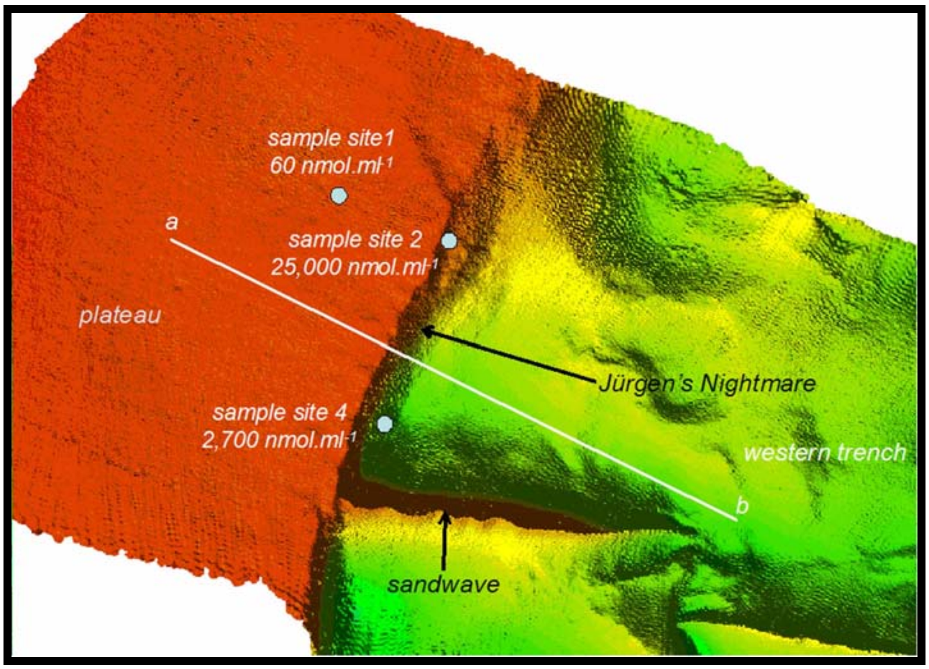

Figure 45: Sample sites and methane concentrations in sediment porewaters near Jürgen's Nightmare. The location of the seismic profile a-b (Fig. 39) is also indicated.

The only water samples collected were from the eastern trench in 175 m of water. These contained lower concentrations of methane (2.5 to 3.1 nmol l^{-1}), yet all the samples were over-saturated with methane relative to the atmosphere (sea surface sample: 108%).

3.4.2 Texel 11

Interest in this area was originally shown by Croker (1994) because data acquired during a cable route survey, pinger and boomer profiles indicated the presence of shallow gas (Fig. 46). The whole of this area is underlain by potential source rocks of both Dinantian and Westphalian ages (Fig. 2b), the latter sub-cropping beneath the Quaternary sediments (Fig. 3).

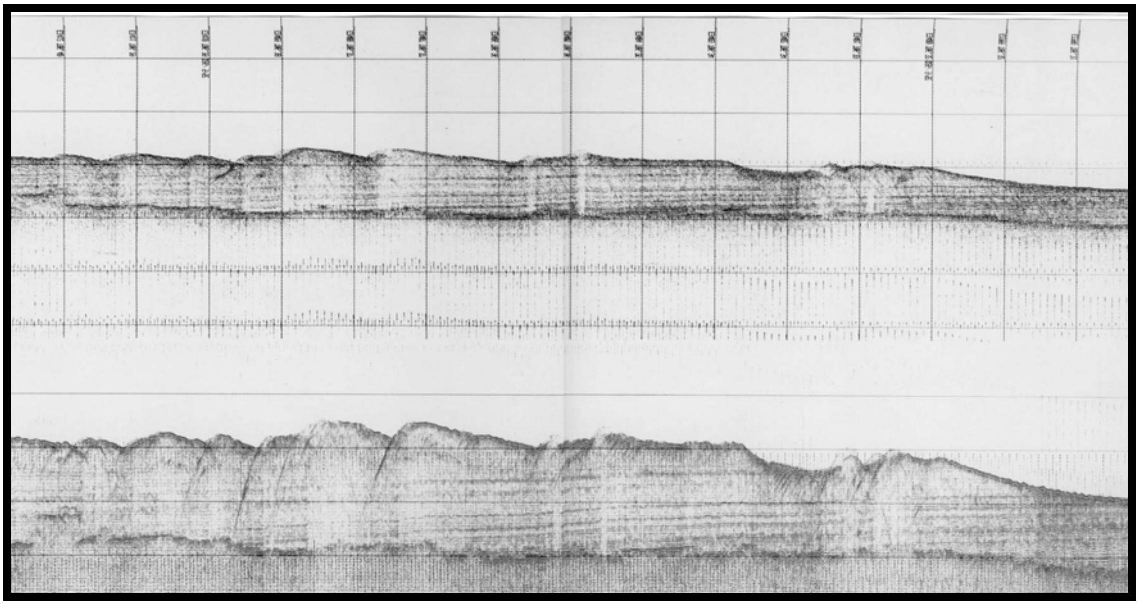

Figure 46: Seismic profiles (pinger above, boomer below) across Texel 11. The inclined reflections represent the Prograded Facies. Vertical columns are believed to be artefacts caused by signal starvation where sand waves occur on the seabed. The irregular reflections towards the bases of the profiles are caused by acoustic turbidity (from Croker 1994).

The seabed in this area is generally flat, except in the north, where small mounds occur, and in the south where a large hollow, 10 to 15 m deeper than the adjacent seabed, extends beyond the survey area (Fig. 47 – overleaf). MBES and side-scan sonar data acquired for SEA6 show that the seabed is characterised by coarse sediments; there are also scattered boulders in some areas (seen on side-scan sonar data as bright targets throwing shadows; see Fig. 48), and mounds apparently composed of boulders (Fig. 49). Superimposed on this coarse seabed are mobile bedforms: sandwaves, sand megaripples etc..

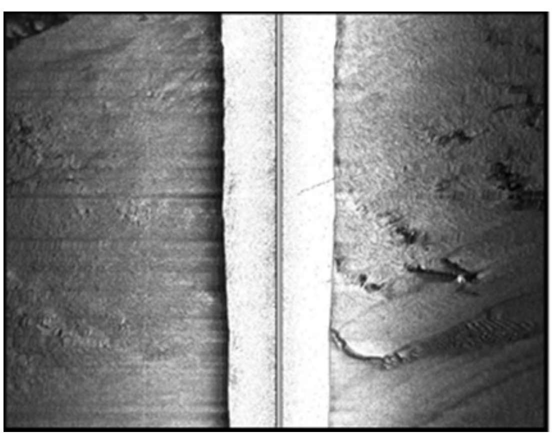

Figure 48: Side-scan sonar image showing scattered boulders on the seabed.

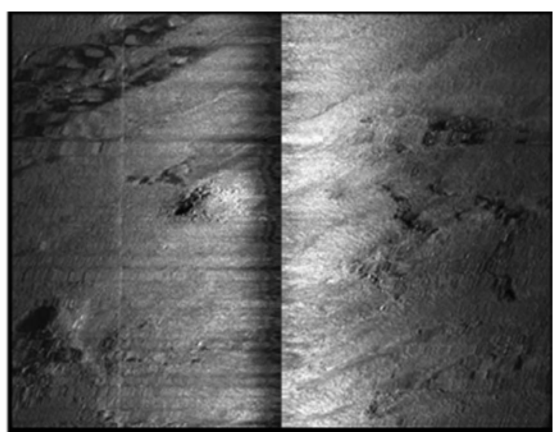

Figure 49: Side-scan sonar image showing boulder-strewn seabed mounds.

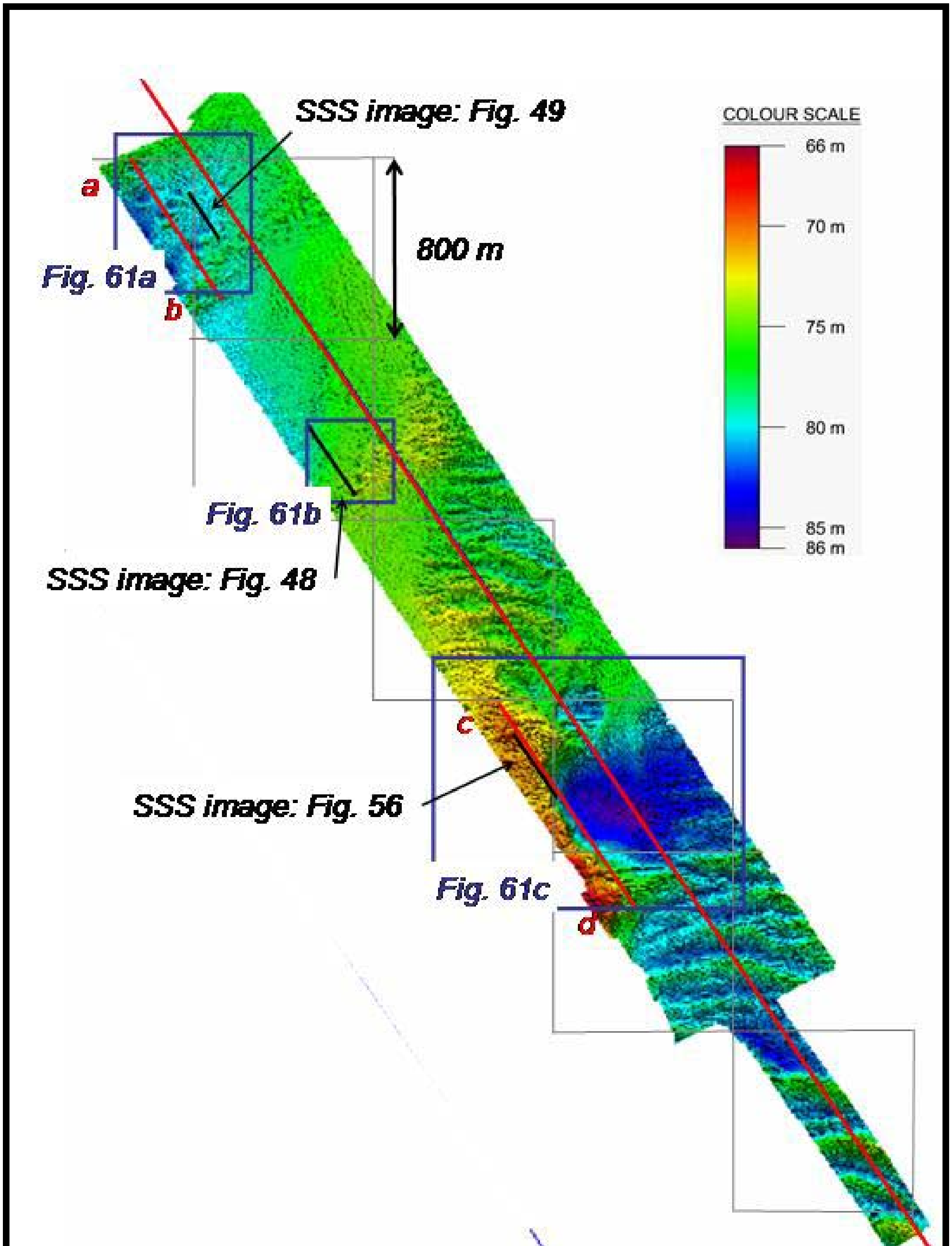

Figure 47: MBES bathymetry of Texel 11. Red lines show the locations of seismic profiles (Fig. 46 - the axial line; Fig. 53 – profile a-b; Fig. 54 – profile c-d); black lines the locations of side-scan sonar images (Figs. 48, 49 and 56); and blue rectangles detailed MBES images (Figs 61a, b and c).

Figure 50: Coarse, shelly seabed sediment.

Photographic surveys and sampling confirmed that over much of the area there are coarse-grained sediments; there is also a significant amount of shell debris (Fig. 50). In places there is rippled sand, often with shell debris (Fig. 51); sand waves are composed of mobile, loose clean sand. It seems that this coarse sediment cover, typical of the current-dominated seabed of the central Irish Sea, overlies a blue-grey clay (Fig. 52).

Figure 51: Rippled sand with shell debris.

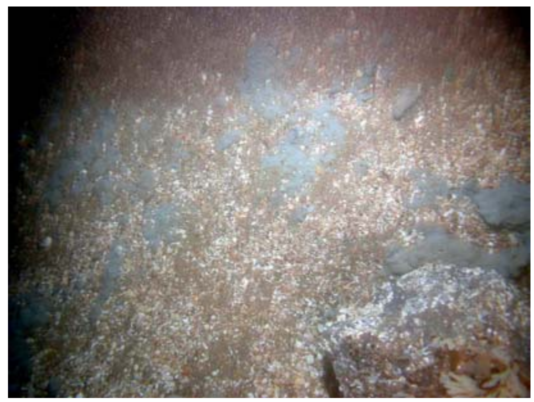

Figure 52: Coarse shelly seabed sediment lying on clay.

Profiler data shows the presence of dipping sub-seabed sediment layers (the late-Quaternary Prograded Facies of the Western Irish Sea Formation) and indicators of gas (reflection enhancement and acoustic turbidity); the dip is towards the north. The configuration of the acoustic turbidity and reflection enhancement ('brightening') suggests that gas is migrating up-dip (i.e. towards the south), periodically stepping from one permeable horizon to another (Fig. 53). The outcrops of one such brightened horizon occurs at the edge of the southern seabed hollow (Fig. 54).

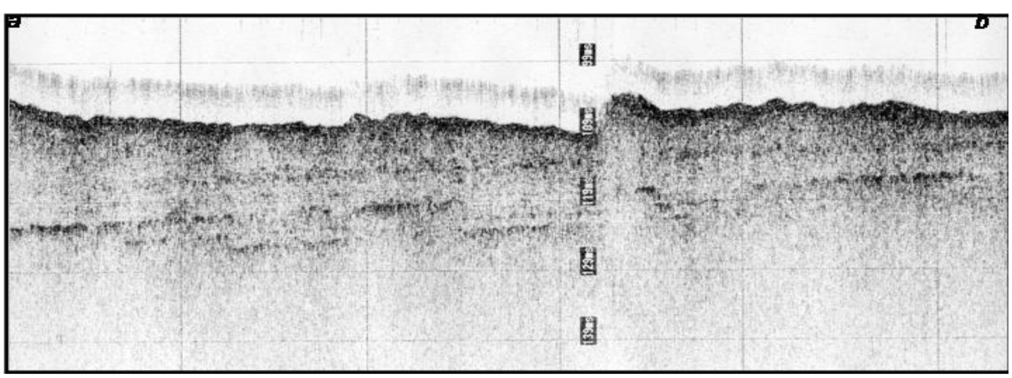

Fig 53: Seismic (chirp) profile; enhanced reflectors indicating the presence of shallow gas.

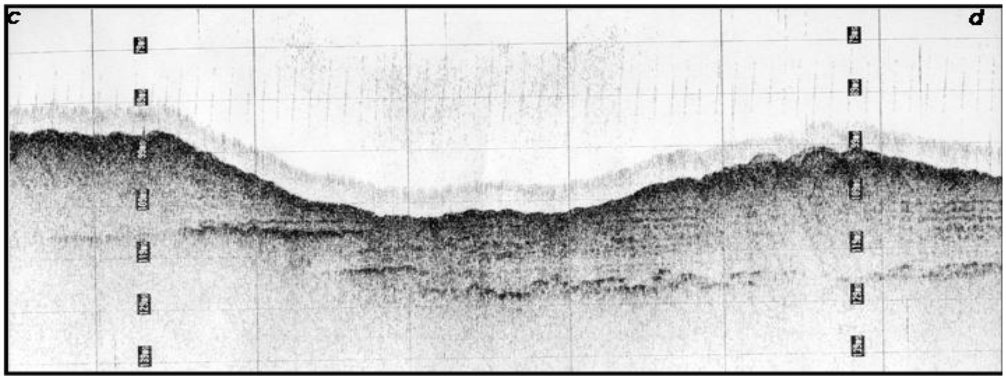

Fig 54: Seismic (chirp) profile; enhanced reflectors (shallow gas) approaching the seabed at the edge of the southern seabed hollow.

Photographic and sampling surveys, guided by the geophysical data, focussed on three areas (Fig. 47). Seven grab samples contained pieces of a hard material comprised of a sandy sediment bound by a cement (Fig. 55). This cemented hard ground forms crusts and blocks standing up to about 1 m above the seabed in all three study areas. In the north it occurs on rocky mounds identifiable on side-scan sonar (Fig. 49), and in the central area and the northern part of the southern area as more-isolated blocks (Fig. 48). The western rim of the southern hollow is composed of a 6 to 8 m-high cliff (see Fig. 47) of this cemented hard ground (Fig. 56). These 'reefs' are colonised by an abundant fauna, including: bryozoans, hydroids, sponges, anemones, starfish, urchins, lobster, and squat lobster (*Munida sp.*).

Fig 55: One of the 'rock' (MDAC) samples collected by grab from the seabed.

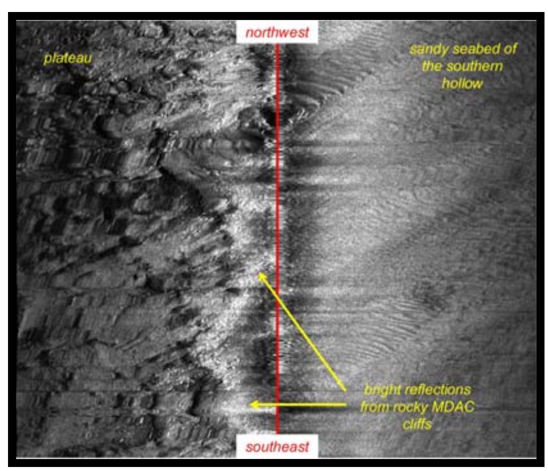

Fig 56: Side-scan sonar (corrected) image of the 'Texel cliffs' at the western edge of the southern hollow (the red line marks the centre of the record). Note the bright reflections caused by the hard (MDAC) material of which the cliff is composed.

A reaction with hydrochloric acid (HCl) indicates that the cement is a carbonate. Examination by scanning electron microscope (SEM) confirmed that the samples are composed of a quartz-dominated sediment bound by a carbonate cement (Figs 57 and 58). X-ray (EDX) analysis (Fig. 59) revealed that the dominant elements present in the cement are calcium (Ca) and magnesium (Mg) along with silicon (Si), suggesting that the cement is composed of a high-magnesium calcite or aragonite; these minerals are commonly associated with MDAC.

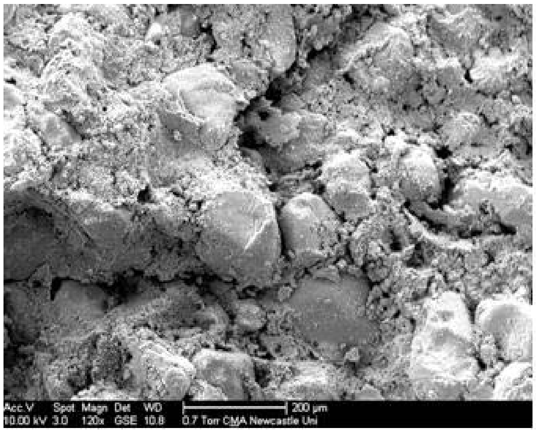

Fig 57: Scanning Electron Microscope (SEM) image (120 x magnification) of an MDAC sample from Texel 11. Note the rounded sand grains held in a fine crystalline cement.

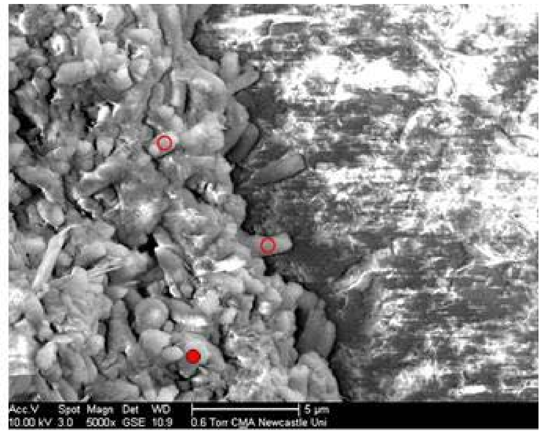

Fig 58: Scanning Electron Microscope (SEM) image (5,000 x magnification) of the same MDAC sample as shown in Fig. 57. The right side of the image is occupied by a sand (quartz) grain, the left by the authigenic cement. The red spot indicates the site of the EDX analysis shown in Fig. 59. EDX analyses at other sites (red rings) provided comparable results.

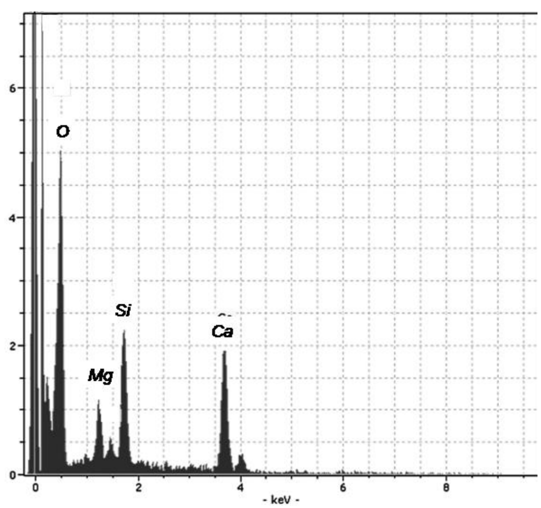

Fig 59: EDX analysis of area around the red spot shown in Fig. 58.

Seven samples of the cemented hard ground were submitted for carbon isotope analysis. $\delta^{13}C$ values indicate that the carbonate of five of these was derived from methane (Fig 60.); the material is methane-derived authigenic carbonate (MDAC).

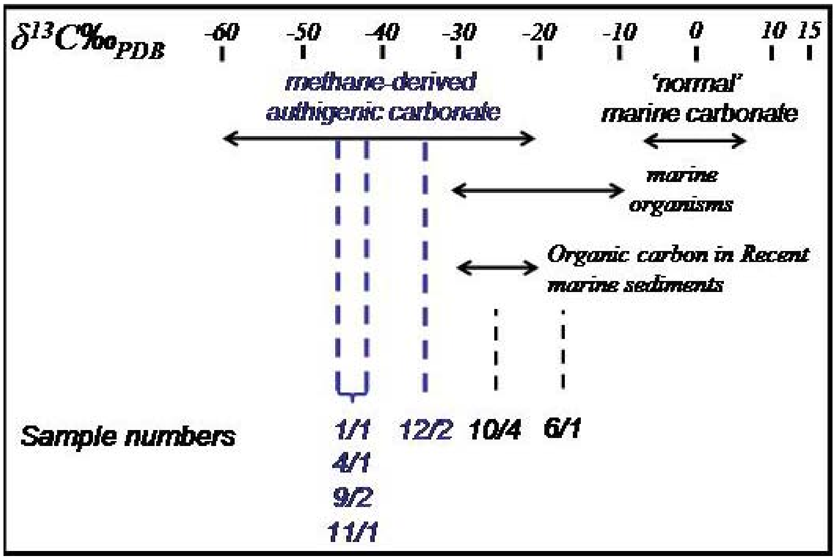

Figure 60: Carbon isotope analyses of samples from Texel 11. All the samples contain methane-derived carbonates (MDAC), along with a proportion derived from other sources (anaerobic breakdown of organic matter to CO2, and seawater carbonate).

The extent of the MDAC reefs is indicated first by the samples of confirmed MDAC, and secondly by the number of photographs on which the hard grounds can be identified (Figs. 61a to c); MDAC seems to be more or less continuously exposed over a distance of at least 500 m in the cliffs on the western edge of the southern hollow (Fig. 61c). Using the character of the seabed as seen on the MBES and side-scan sonar images as a guide, a much greater extent of MDAC exposure is suggested (Fig. 62); clearly the MDAC also extends beyond this study area, but it seems that MDAC may be present, but not continuous, over an area of >500,000 m^2; not all of this may be exposed at the surface.

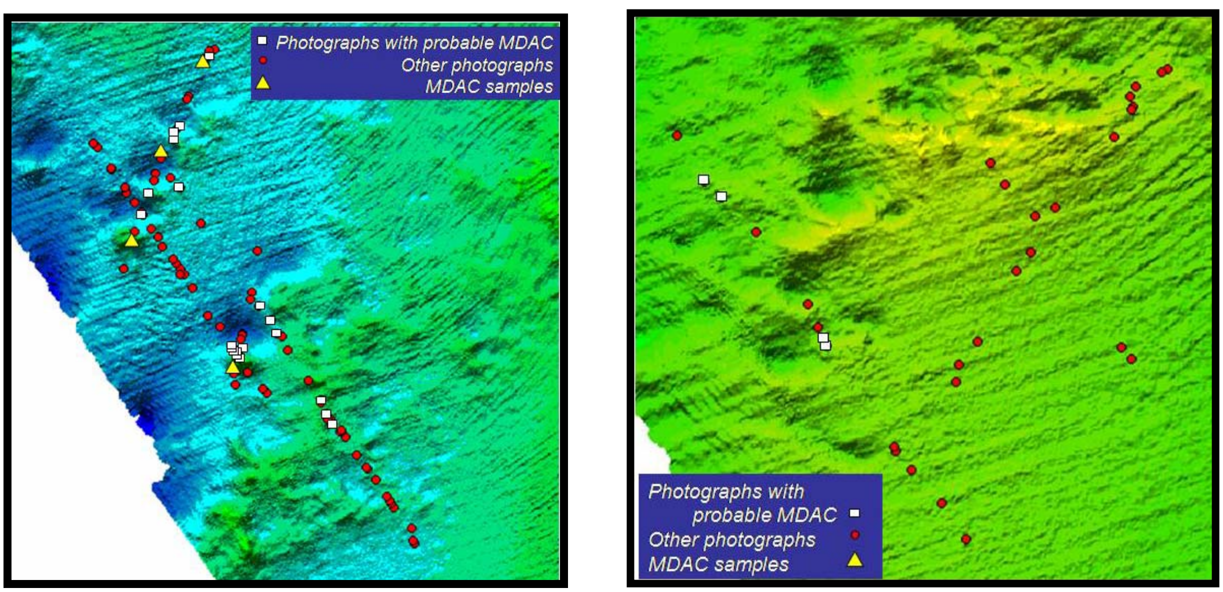

Figure 61: Distribution of confirmed MDAC samples and photographs of unconfirmed MDAC. Figure 47 shows the locations of the three areas a) above left; b) above right; c) next page.

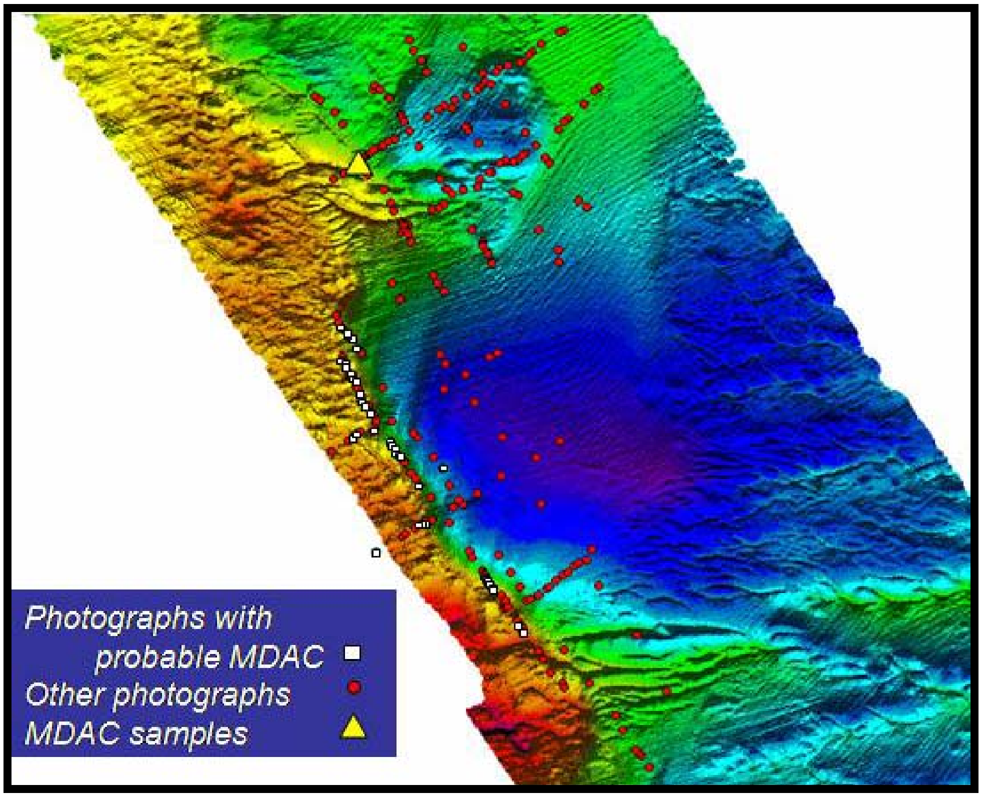

Figure 61c: for caption see previous page.

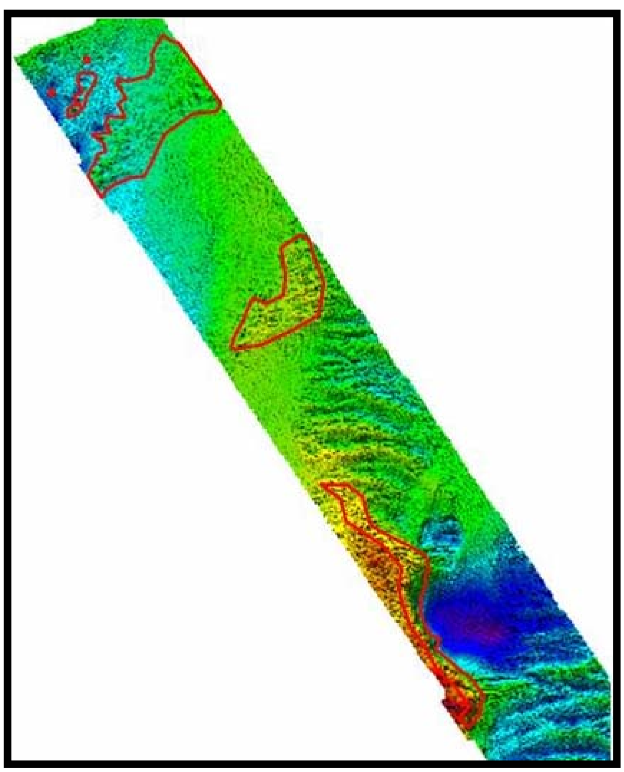

Figure 62: Anticipated extent of MDAC in the Texel 11 survey area (indicated in red).

3.4.3 Texel 10

As at Texel 11, seismic (pinger and boomer) profiles acquired during a cable route survey indicate acoustic turbidity within gently-inclined, seismically-layered, strata of the Prograded Facies of the Western Irish Sea Formation (Fig. 63). This area is underlain by potential source rocks of Dinantian age (Fig. 2b); the western end is also underlain by potential source rocks of Westphalian age (Fig. 2b) which sub-crop beneath the Quaternary sediments (Fig. 3).

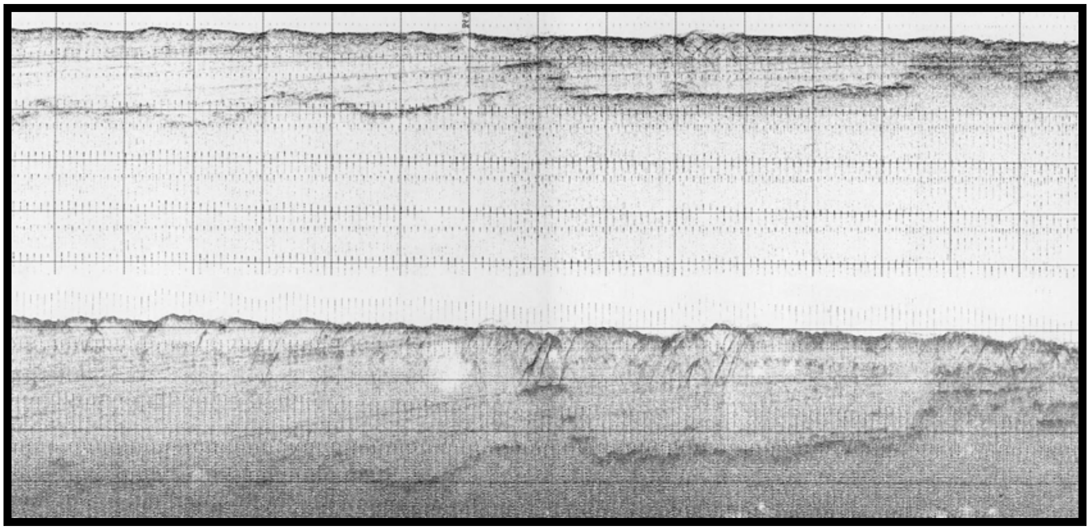

Figure 63: Acoustic turbidity rising beneath seabed in coarse-grained sediments at Texel 10; above: pinger; below: boomer (from Croker 1994).

MBES data acquired for SEA6 shows that the area centred on Fig. 63 has an irregular topography with some sand waves and megaripples, and large seabed hollows (Fig 64).

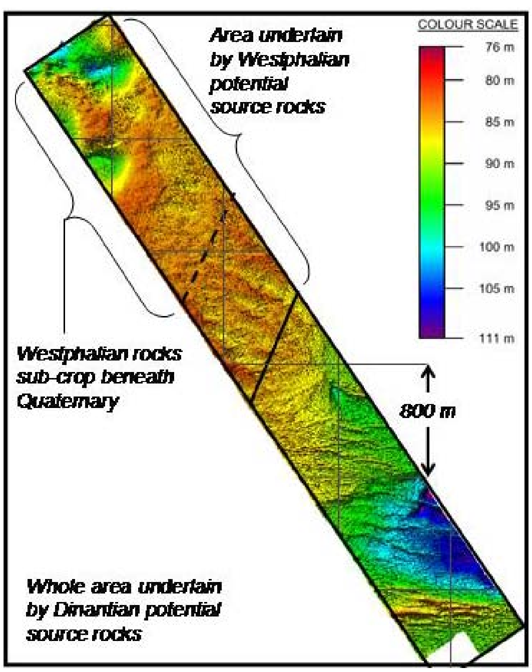

Figure 64: MBES bathymetry of the Texel 10 survey area; the areas underlain by potential source rocks are indicated.

Photographic surveys and sampling showed that the sand waves are composed of clean sand (Fig. 65), and that the intervening seabed is generally covered by coarse-grained sediments, with varied concentrations of sand, shelly material, pebbles, and cobbles (Fig. 66). In some places a blue-grey clay is exposed beneath the surficial sediments (Fig. 67). The coarseness of the seabed sediments in the northern-most seabed hollow seems to scatter acoustic energy; there are no reflections from sub-seabed sediment layers here (Fig. 68).

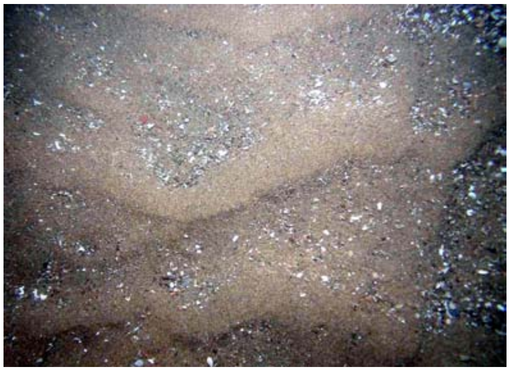

Figure 65: Rippled sandy seabed sediment; clean sand with small shell fragments.

Figure 66: Sandy seabed sediment with abundant pebbles and cobbles, and shell fragments.

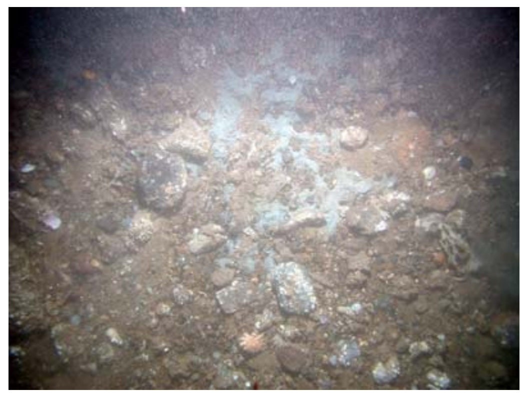

Figure 67: Coarse seabed sediment (dominated by pebbles and cobbles) overlying blue-grey clay.

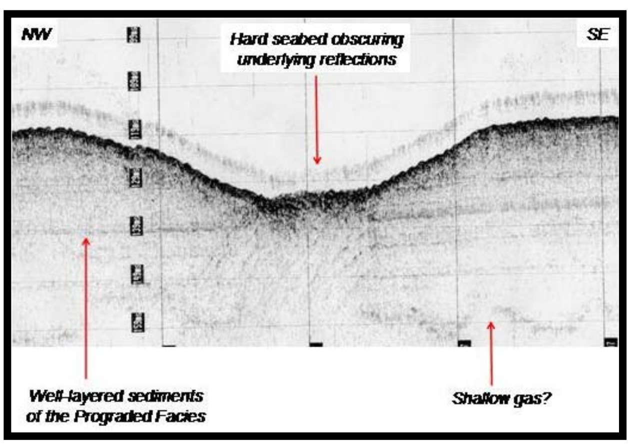

Figure 68: Seismic (chirp) profile across the northwest hollow. Layered sediments of the Prograded Facies are visible, except where the coarse seabed sediment within the hollow prevents penetration by the acoustic signal. [Location indicated on Fig. 69.]

The inherent variability of the seabed sediment, and the abundance of shells and stones on the surface, made grab sampling, difficult. Clay samples proved to be firm to stiff, and silty.

Acoustic turbidity and reflection enhancement on seismic profiles indicate that shallow gas underlies most of the survey area, but both the depth beneath the seabed and the reflection amplitude are variable (Fig 69). In places the gas steps upwards between sediment layers (Fig. 70).

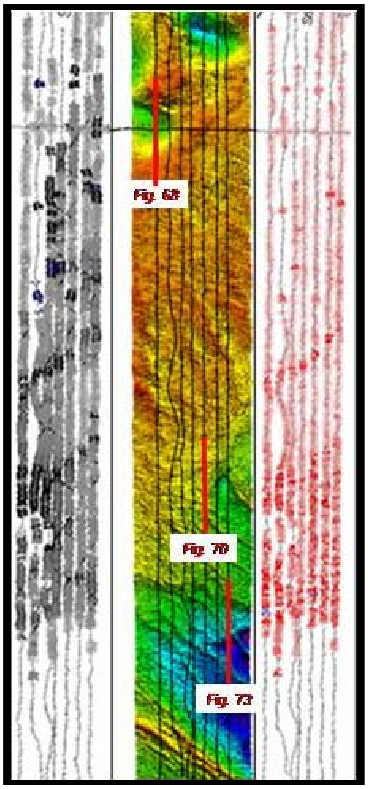

Figure 69: The distribution of shallow gas (acoustic turbidity and enhanced reflections) at Texel 10: Left: depth to gas (colour intensity increases towards the seabed); Centre: MBES bathymetry showing seismic survey lines; Right: brightness (amplitude) of enhanced reflections. The locations of Figs. 68, 70, and 73 are indicated.

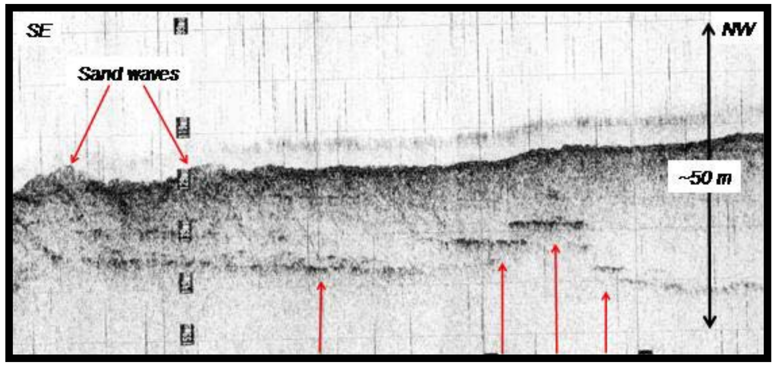

Figure 70: Seismic (chirp) profile showing reflection enhancement (arrowed) stepping between layers in the Prograded facies. [Location indicated on Fig. 69.]

Methane concentrations in sediment porewaters (Fig. 71) are relatively high. Water samples collected from this area had methane concentrations within the range 2.4 to 4.8 nmol.l^{-1} (see Fig. 72). As concentrations were lower close to the seabed, there is no evidence of a strong seabed methane source; however, the strength of the bottom currents encourages rapid mixing and dilution, and would make it very difficult to sample localised sources.

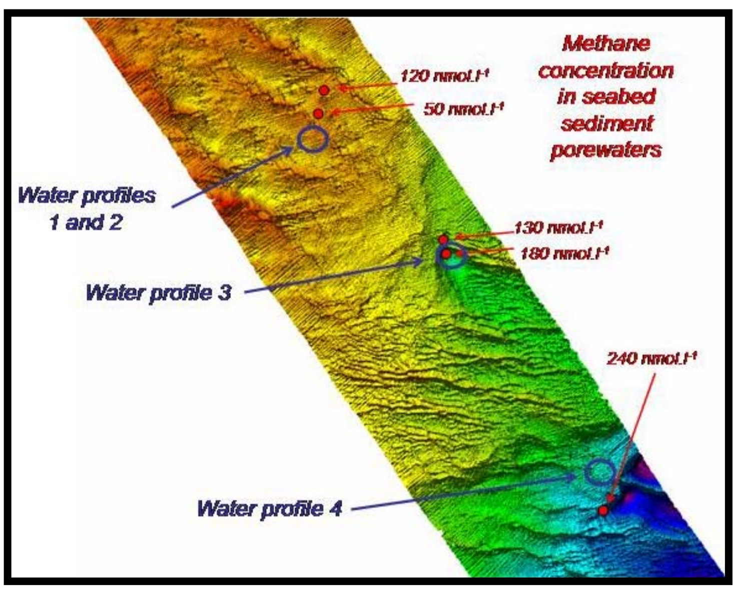

Figure 71: Methane concentrations in the porewaters of seabed sediments. The water profiles indicated are shown in Fig. 72.

Figure 72: Methane concentrations in seawater. The locations of the four profiles are indicated on Fig. 71.

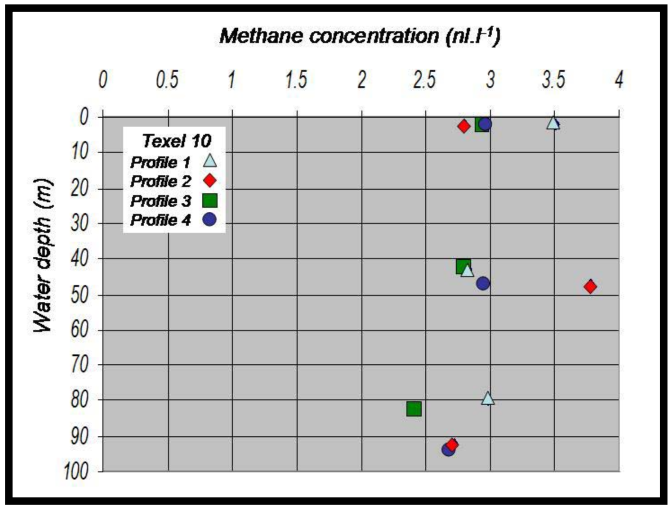

The seabed hollows seem to occur where the topmost sediment layers have been truncated by erosion. The northern rim of the large hollow in the southeast of the survey area, for example, is marked by a steep slope (Fig. 73); a 10 m vertical drop over 24 horizontal metres. The northwest edge of the smaller hollow (where water profile 3 was collected – see Fig. 71) has a drop of 5 m over a 16 m horizontal distance.

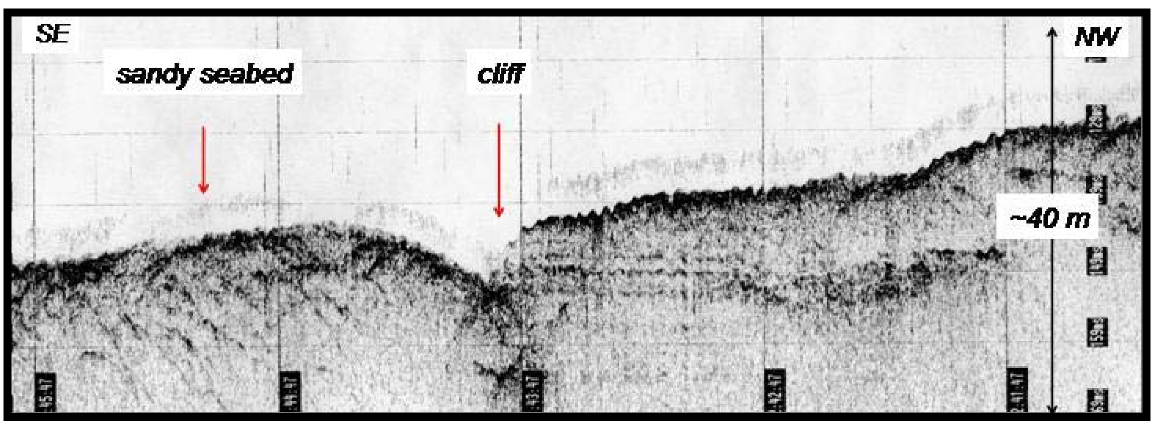

Figure 73: Seismic (chirp) profile crossing the 10 m-high cliff at the northern edge of the seabed hollow in the southeast of the Texel 10 survey area. Note the enhanced reflections (indicating shallow gas), and the layering in the sediments of the Prograded Facies, which is truncated in the cliff. [Location indicated on Fig. 69.]

At the cliff tops, slabs of a light brown rock are exposed (Fig. 74). Although no samples of this material have been collected, it is speculated that this brown rock is a coarse layer within the generally clayey Prograded Facies sediments. Such coarse layers are consistent with the acoustic layering seen on the seismic profiles, and enhancement of reflections representing such layers could be explained as gas accumulating within them. Layers of blue-grey clay are exposed in the cliffs (Fig. 75), and blocks of clay accumulate at the base of the slopes (Fig. 76).

Figure 74: Slabs of light brown rock, apparently conformable with the underlying blue-grey clay of the Prograded facies, exposed at the top of the 10 m-high cliff at the northern edge of the seabed hollow.

Figure 75: Blue-grey clay of the Prograded Facies exposed at the top of the 10 m-high cliff. The clay is covered by a thin veneer of coarse sand.

Figure 76: Blocks of clay accumulating at the base of the cliff.

Considering that the Prograded Facies is described as of late-Pleistocene age (Jackson *et al*., 1995), it is surprising firstly that it has acquired sufficient tensile strength to fracture like a rock, secondly that it can form such steep underwater cliffs, and finally that so much erosion has occurred since the late Pleistocene (albeit less than in Harvey Trench). As no suitable samples were collected during the SEA6 surveys, it is impossible to tell whether or not this strength is provided by a methane-derived carbonate cement. However, the presence of gas beneath the seabed, and the relatively high methane concentrations in the sediment porewaters suggest that this possibility cannot be ruled out.

3.5 The Codling Fault

The Codling Fault is a major strike-slip fault extending from the Kish Bank Basin, near the Irish Coast, south-east towards Cardigan Bay (Fig. 35). It has a complex fault zone several kilometres wide (Jackson *et al.*, 1995; Croker, Garcia-Gil *et al.*, 2002); recent minor earthquakes suggest that the fault is still active (Croker, Garcia-Gil *et al.*, 2002).

Croker, Garcia-Gil *et al.* (2002) reported that, within the Irish sector, there are several features indicative of seabed fluid flow in the fault zone. These include seabed mounds (e.g. Fig. 77), one of which is clearly seeping gas (Fig. 77 inset). Video evidence, supported by samples, suggests that MDAC is present on these mounds. This evidence links the Codling Fault with the migration of fluids, probably from underlying Carboniferous strata.

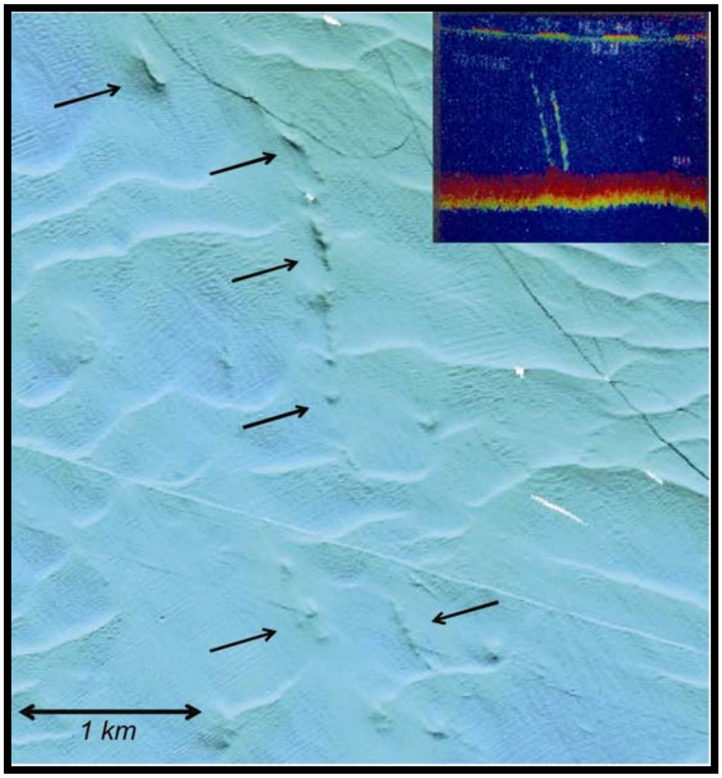

Figure 77: MBES image showing seabed mounds associated with the Codling Fault (Irish Sector) Inset is a bridge echo sounder image showing seep plumes rising from one of the mounds (from Croker, Garcia-Gil *et al.*, 2002).

Surveys were undertaken as part of the SEA6 project to investigate the extension into U.K. waters of the influence of the Codling Fault on seabed fluid flow and MDAC formation.

3.5.1 Codling Extension

A 15 km long area approximately 1 km wide and aligned North-South was surveyed adjacent to the UK/Irish median line. The general seabed depth ranges from 90 m in south to 130 m in the north (Fig. 78 - overleaf). At both the northern and southern ends of the survey area the seabed is characterised by sand waves <4 m high and <20 m wide. However, the dominant features are large sand waves about 25 m tall, <200 m across and <750 m long. A NNE-SSW line of these features extends across most of the area. Individual sand waves are 300 to 500 m apart and aligned WNW-ESE. Photographs and samples show that these sandwaves are composed of coarse sand. They are clearly active: sediment movement obscured vision during the photographic surveys. Also, during calm weather current effects were visible above the sandwaves (Fig. 79), and after a gale the surface water was discoloured by fine sediment. There are deep scour hollows at the ends of the sand waves.

Figure 79: Sea surface effects caused by strong tidal currents over the sand waves of Codling Extension (water depth ~100 m). Photographed from S/V *Meridian* during the SEA6 geophysical survey.

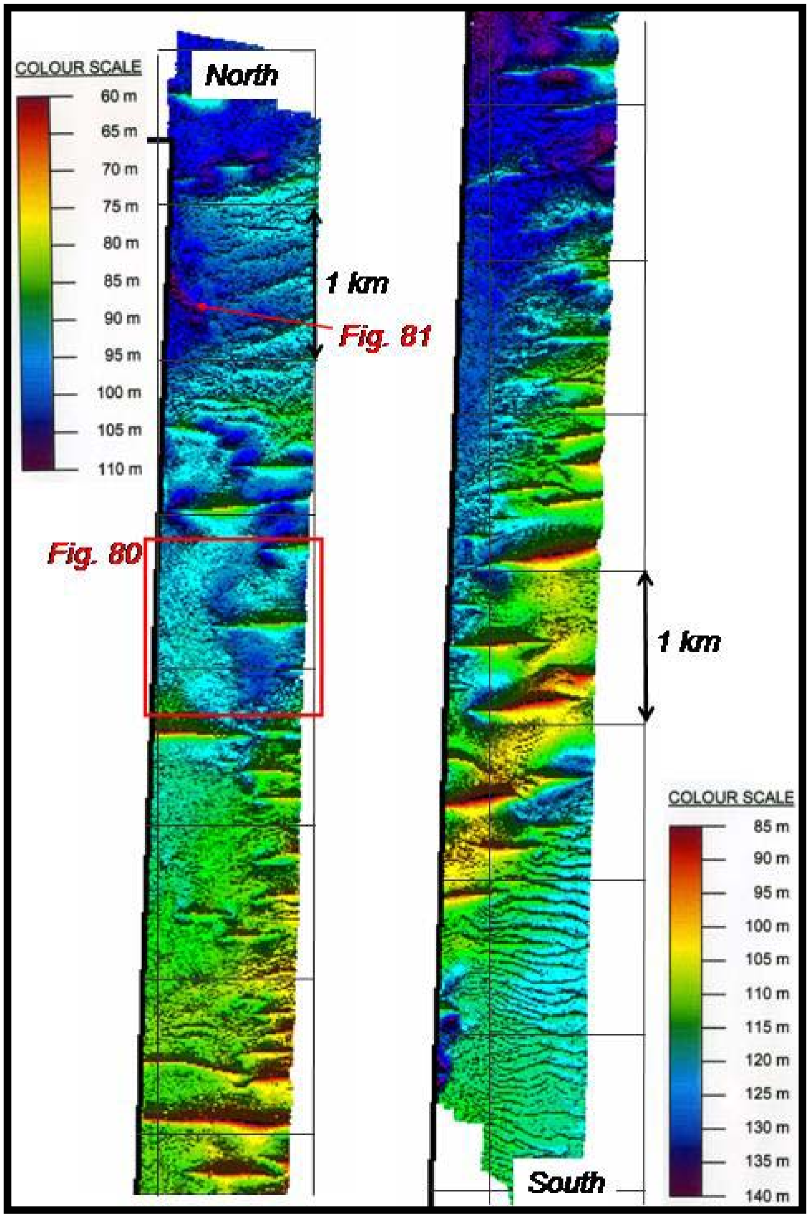

Figure 78: MBES bathymetry of the Codling Extension survey area; northern half on the left, southern half on the right [note the separate depth scales].

The MBES bathymetry revealed no features which seem directly associated with seabed fluid flow; however, there are lineations and of depressions, features which may be indicative of seabed displacement (Fig. 80) some of which were investigated.

Photographic traverses of the central part of the survey area showed that much of the seabed is generally sandy, and swept by tidal currents strong enough to entrain a considerable bed load; sand grains, as well as shell material (e.g. whole gastropod shells), were seen moving across the seabed. Over the sandwaves visibility was reduced to zero by mobile sand, even several metres above the seabed. The sediments in the depressions is very coarse, comprising pebbles, cobbles and boulders (Figs. 81 and 82). Rock samples (e.g. basalt) proved to be solid rock, presumably derived from sediments from which the finer material had been removed by the current.

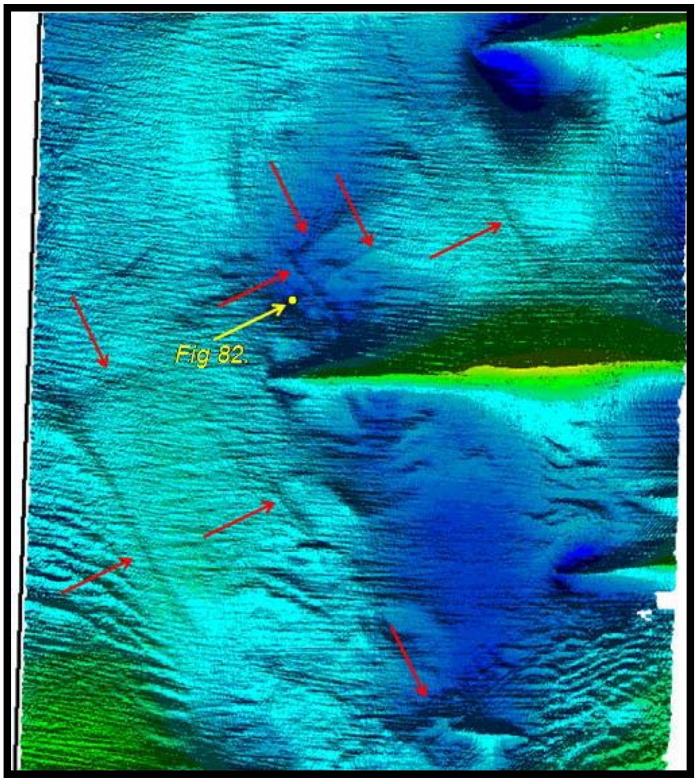

Figure 80: Detailed MBES bathymetry of part of the northern Codling Extension area. The red arrows indicate apparent seabed lineations, arranged in a rectilinear pattern.

Fig 81: Seabed boulder in a deep (>135 m) trench (see Fig 79. for location). Visibility is reduced by water-borne sand-sized particles.

Fig 82: Coarse (pebble and cobble-sized) seabed Sediments (see Fig. 80 for location).

The coarse seabed sediment was impenetrable by the chirp profiler used on the SEA6 surveys, so it is impossible to comment on whether or not there is any shallow gas. If there is any seabed fluid flow in this area, the evidence of it is obscured by the coarse, mobile sediment, and the vigour of the bottom currents.

Two attempts to deploy water bottles failed because of the strength of the current. Methane concentrations (2.8 $nmol.l^{-1}$) in samples taken from the sea surface were high relative to the atmosphere (120% saturation).

3.6 Cardigan Bay

The majority of Cardigan Bay is not well supplied with potential methane sources apart from a few areas of fine-grained Holocene sediments (Fig. 2a). Areas of shallow gas off Newquay and Tywyn, in the south and centre of the Bay respectively, were indicated by Hession (1988), otherwise indications of seabed fluid flow are confined to the more widespread shallow gas in Tremadog Bay (Fig. 4) identified by Taylor-Smith (1987) and Hession (1988). These gassy sediments are not confined to muddy areas, and some muddy areas have no previously reported acoustic turbidity. Taylor-Smith provided an illustration (Fig. 83) which suggests a relationship between acoustic turbidity and peat; the extent of the acoustic turbidity (according to Taylor-Smith) seems to correlate with the extent of Mid-Oligocene to Lower Miocene lignites identified by BGS (see Fig. 2b). These lignites sub-crop beneath the surficial sediments (Fig 3).

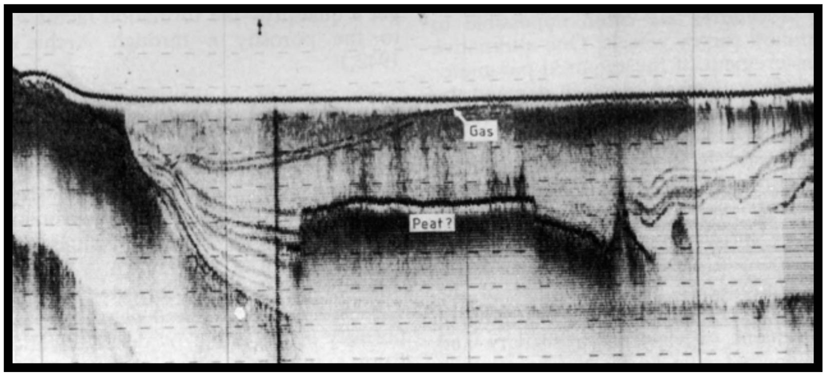

Figure 83: Acoustic turbidity in Tremadog Bay (Reproduced by permission of The Geologists' Association from Proceedings of the Geologists' Association, D. Taylor Smith, Geotechnical studies in Tremadog Bay, 98, 385-396. © 1987 The Geologists' Association**).**

No further evidence suggesting the presence of MDAC has been published, but an unpublished report from the Countryside Council of Wales (CCW) concerned a rocky reef off Barmouth. This reef (Holden's Reef), and the gassy sediments of Tremadog Bay were covered by the SEA6 surveys conducted from S/V *Lia* (Osiris Projects, 2005); the survey coverage is shown in Fig. 84.

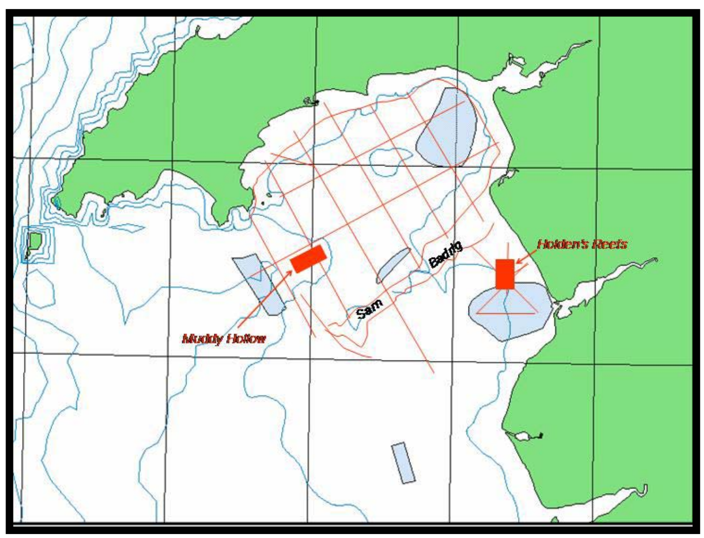

Figure 84: SEA6 surveys undertaken on S/V Lia. Geophysical survey lines are shown in red; red blocks show detailed survey coverage of Muddy Hollow and Holden's Reefs. Previously mapped extent of acoustic turbidity (shallow gas) is marked with a light blue ornament.

3.6.1 Tremadog Bay

The SEA6 seismic surveys of Tremadog Bay confirmed the presence of acoustic turbidity (shallow gas), but indicated that it is more widespread than previously thought. Sediment porewater analyses (Appendix II) show that methane concentrations in, and close to, areas of acoustic turbidity in Tremadog Bay and Muddy Hollow are high compared to both atmospheric concentrations and to concentrations in the deeper waters of the central Irish Sea and Western Mud Belt. Comparison with the extent of the two potential methane sources in the area (Fig. 2), suggests that the fine-grained Holocene sediments are responsible for the gas in Muddy Hollow, but that the Oligocene-Miocene lignites account for the majority of the gas distribution (Fig. 85). As survey coverage does not extend throughout the area underlain by the lignites, it is anticipated that shallow gas is even more widespread.

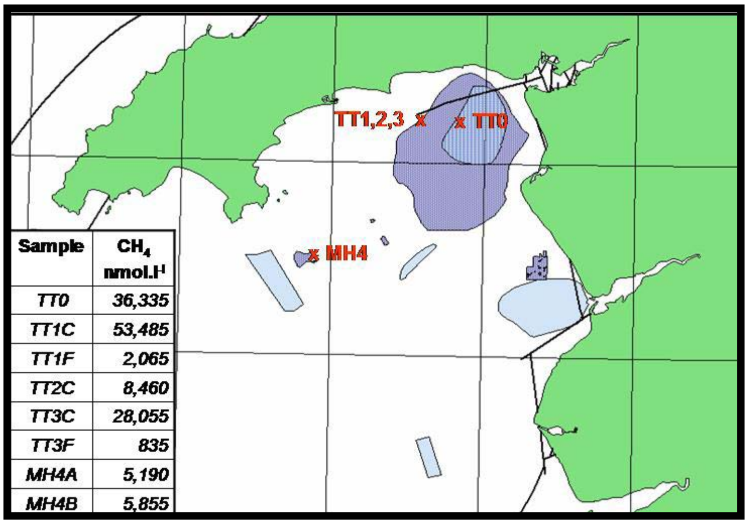

Sample	CH_4 nmol.l^{-1}
TT0	*36,335*
TT1C	*53,485*
TT1F	*2,065*
TT2C	*8,460*
TT3C	*28,055*
TT3F	*835*
MH4A	*5,190*
MH4B	*5,855*

Figure 85: The distribution of shallow gas in Tremadog Bay. The light blue ornament shows the previously reported distribution; the darker blue the distribution mapped by the *Lia* surveys. Sample locations and numbers are shown in red; concentrations of methane in sediment pore waters are shown on the inset table, and in Appendix II.

The shallow gas in Muddy Hollow seems to be associated with fine-grained Holocene sediments. Elsewhere the shallow gas seems to be associated with Oligocene-Miocene lignites.

3.6.2 Holden's Reefs

A topographic feature off Barmouth, marked on the Admiralty Chart as an 'obstacle', was found to comprise a rocky reef when investigated by CCW divers. During the *Lia* operations a detailed geophysical grid around the CCW dive site was surveyed to determine the nature and extent of this 'reef'. Results, presented and discussed by Osiris Projects (2005), show features with a strong acoustic response on side-scan sonar (Fig. 86) and seismic profiler (boomer) records (Fig. 87) at the CCW site, and extending to cover a considerable area (Fig. 88). There are numerous individual features ranging in size from about 1m to 100 m across. Generally these features, which lie within an area characterised by fine sands, have little topography, but in places individual structures stand up to 1.5 m above the seabed.

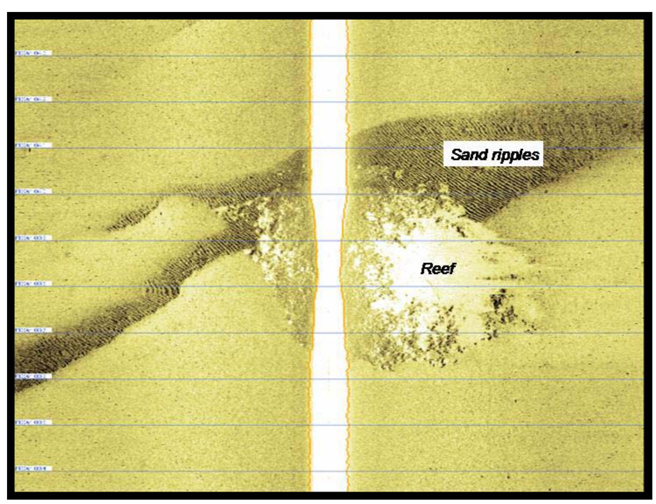

Figure 86: Side-scan sonar record showing part of Holden's Reefs (from Osiris Projects, 2005).

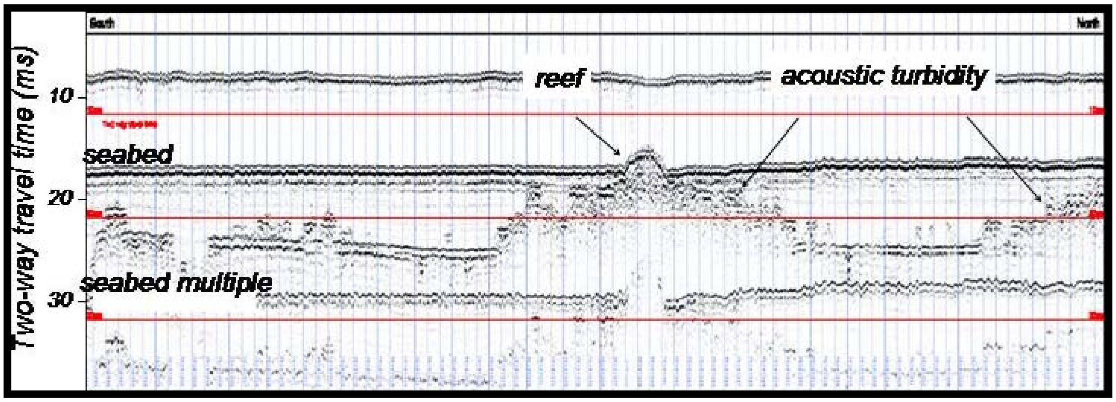

Figure 87: Seismic (boomer) profile of part of Holden's Reefs, showing extensive acoustic turbidity (shallow gas) associated with the reef Reefs (from Osiris Projects, 2005).

Seismic profiles suggest that acoustic turbidity is present throughout the area, apart from two small 'windows', and that it rises towards the seabed in the vicinity of the reefs. The interpretation of this acoustic turbidity as gas is supported by divers' reports of gas bubbles rising from the seabed (Fig. 89), particularly during low spring tides. Analyses of the seabed sediment porewaters samples indicated high methane concentrations; the highest value (~5.8 $mmol.l^{-1}$, i.e. 264 x 10^6% saturation) being exceptional.

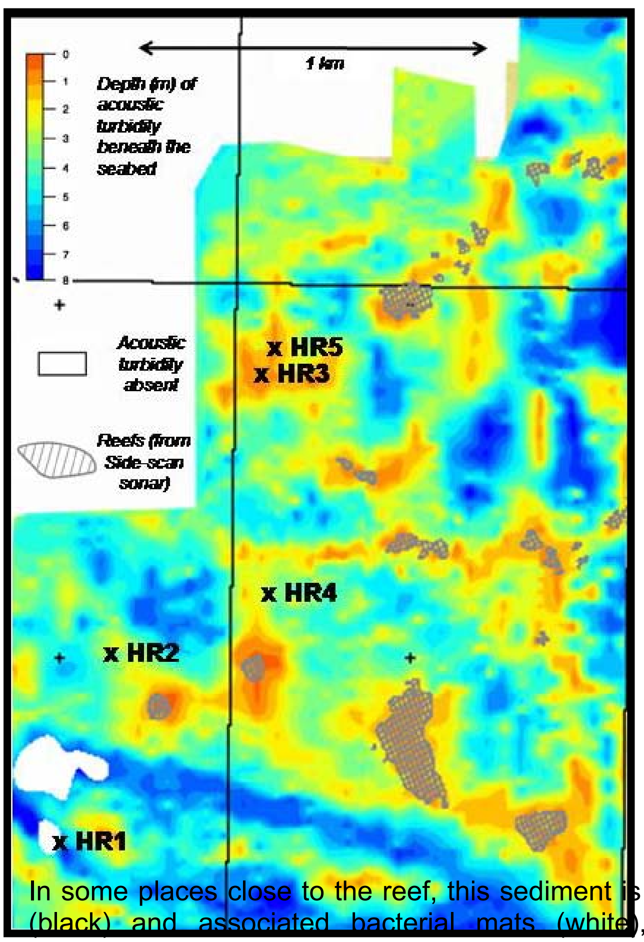

Figure 88: The distribution of Holden's Reefs and shallow gas. [Note: there seems to be a contouring bias associated with the survey line orientation.] Seabed sediment sample locations are indicated. Methane concentrations of porewaters are shown below and in Appendix II:

Sample	Methane concentration $nmol.l^{-1}$
HR1C	560
HR2C	5,796,825
HR2F	51,210
HR3D	33,780
HR3E	3,560
HR4D	133,830
HR4E	48,400
HR5A	9,465

During visual surveys (by CCW divers and photographic surveys from R/V *Lia*) the reefs are seen to comprise hard material colonised by a variety of benthic fauna (Fig 90). They contrast markedly from the normal seabed sediment.

In some places close to the reef, this sediment is discoloured by the presence of sulphides (black) and associated bacterial mats (white), assumed to be the sulphide-oxidiser

Beggiatoa (Fig. 91). Hydrogen sulphide and *Beggiatoa mats* are common features of sites of anaerobic oxidation of methane; another by product of this process is MDAC (Judd, 2001).

Figure 89: Gas bubbles rising from the seabed, Holden's Reefs (photograph courtesy of CCW).

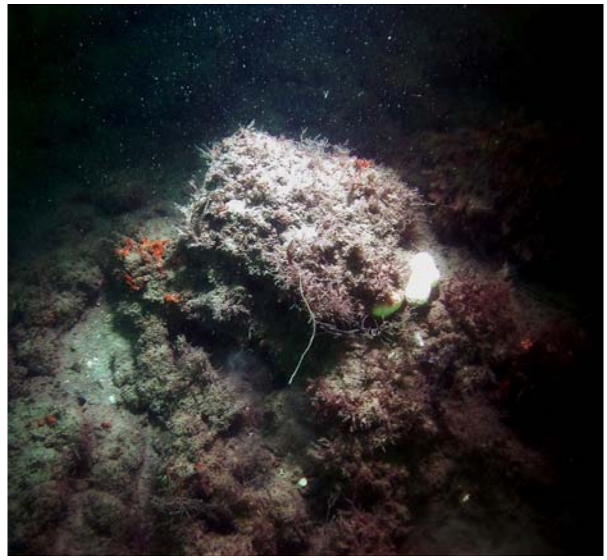

Figure 90: Part of Holden's Reefs.

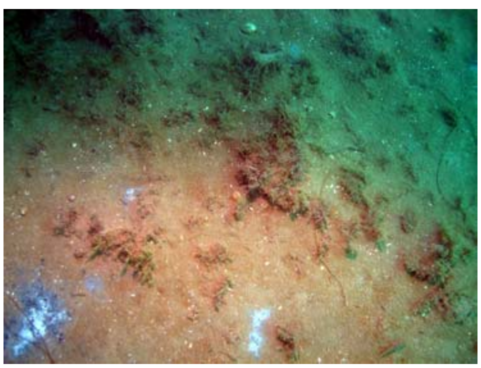

Figure 91: Seabed sediments; bottom left: possibly discolouration caused by the presence of iron(II) sulphide (black) and bacterial mats, probably the sulphide-oxidiser *Beggiatoa* (white).

Inspection by scanning electron microscope (SEM) showed that the reef material is composed of a relatively coarse-grained quartz particles held in a cement (Fig. 92) with high calcium and magnesium contents (Figs. 93 and 94). The EDX analyses are consistent with the carbonate minerals high-magnesium calcite and aragonite.

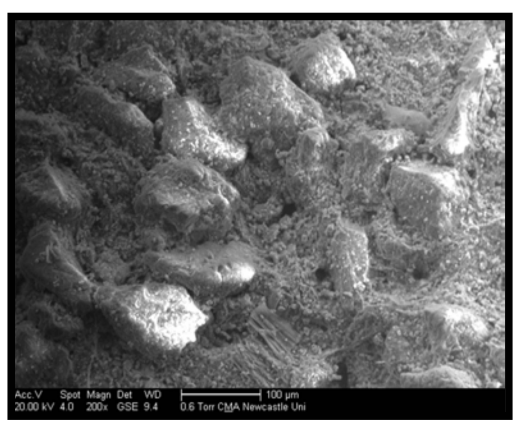

Figure 92: SEM image (200 x magnification) of a sample of reef material showing sub-rounded sand (quartz) grains of held in a fine, crystalline matrix.

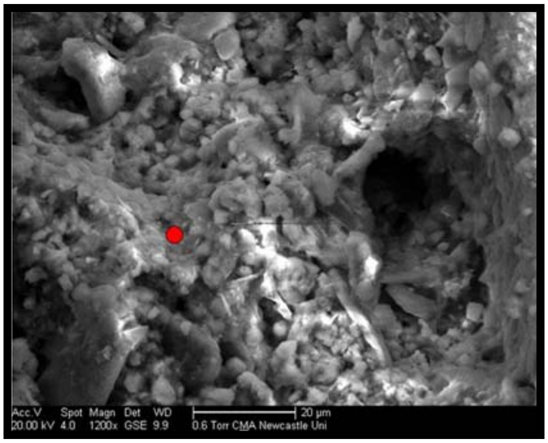

Figure 93: SEM image (1200 x magnification) of the reef cement. The red spot indicates the location of the EDX analysis illustrated in Fig. 94.

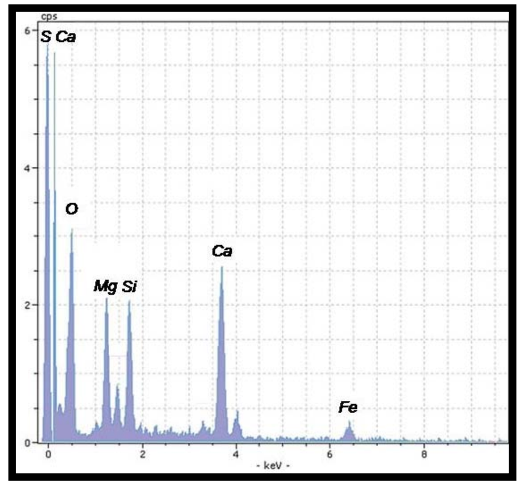

Figure 94: EDX analysis of the location indicated in Fig. 93.

Together, these indicators suggest that Holden's Reefs are composed of methane-derived authigenic carbonate; confirmation comes from the carbon isotope analysis of a single sample taken from the reef by CCW; the $\delta^{13}C$ value of $-33.9‰_{PDB}$ lies within the range of values expected for MDAC (see Fig. 60).

The source of the gas is uncertain, but it seems likely that it comes from the Oligocene-Miocene lignites. The Mochras Fault (Fig. 85), which defines the edge of the Cardigan Bay Basin in which the lignites were formed, or faults associated with it, may influence gas migration.

The mapping undertaken on the *Lia* has shown that Holden's Reefs are far more extensive than previously appreciated. There are 12 reefs and reef clusters, of which the largest, 150 m wide and 350 m long, covers an area of about 10,000 m^2. In total reef structures cover almost 40,000 m^2 of the 3.5 km^2 survey area; there is also at least one small reef outside this survey area.

3.7 Other Areas

3.7.1 Pembroke Carboniferous belt

At the southern limit of the SEA6, potential source rocks of Carboniferous (Dinantian and Westphalian) age are present in a belt extending west from the Pembrokeshire coast (Fig. 2b); in places they sub-crop beneath the surficial sediments (Fig. 3). However, no evidence of shallow gas, seeps, or other indicators of MDAC have been reported from this area.

3.7.2 St George's Wall

Further north Oligocene and Cretaceous sources are present (Fig. 2b). In the same area, astride the UK/Irish median line, lies the most significant salt structure of the whole SEA6 area. This 'salt wall' is described by Tappin *et al* (1994) as being at least 50 km long and in places >3 km wide. It is associated with a major fault, the St George's Fault (hence it is referred to herein as 'St George's Wall'), an *en échelon* prolongation of the Bala Fault, a major structural feature of Cardigan Bay and onshore Wales. This fault and the salt wall mark the limit of a major basin of deposition, the St George's Channel Basin, which contains potential source rocks of Cretaceous age. It seems likely that fluid migration and seepage are associated with it. The absence of evidence to support this speculation may be explained by an absence of suitable (recent) data; however, site survey data produced in 1978 indicated the presence of two diapiric features rising towards the seabed, and anomalous seabed features. The salt wall lies beyond the reach of the SEA6 geophysical surveys, and seabed photographs taken during sea trials at the start of the SEA6 photographic/sampling survey provided no more than evidence of a coarse shelly sediment on a current-swept seabed (Figs. 95 and 96). Nevertheless, the area above and around the St George's Wall remains an area with a high potential for MDAC formation.

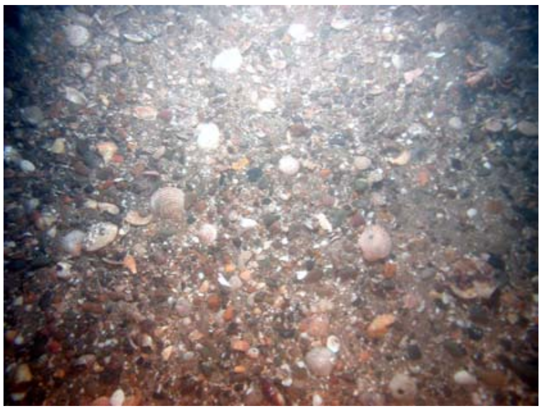

Figure 95 and 96: Coarse seabed sediment, St George's Wall.

3.7.3 Caernarfon Bay

Gas seeps were recorded in Caernarfon Bay by Wingfield (1990), but the evidence for them has not been published. A geophysical reconnaissance survey of the indicated area, undertaken during the SEA6 project, revealed no evidence of shallow gas, gas seeps, or seabed features that might be associated with gas seepage.

The occurrence of potential source rocks of Carboniferous (Westphalian) age beneath part of Caernarfon Bay (Fig. 2b) suggests that gas seepage is possible, particularly where this potential source is covered only by surficial sediments (Fig. 3). However, the BGS seep location lies outside these parts of the bay.

3.7.4 North Channel

Parts of the North Channel are underlain by potential source rocks of Carboniferous (Westphalian and DInantian) age (Fig. 2b). No data suitable for revealing evidence of seabed fluid flow or MDAC have been available during the compilation of this report; however, there is the potential for MDAC formation in these areas.

3.7.5 Firth of Clyde

Although there are no reports of gassy sediments in the SEA6 area in or north of North Channel, Farrow (1983) reported 'proto-dolomitic concretions' formed around the burrows of crustaceans off Greenock and on the shore at Hunterston on the Firth of Clyde. The descriptions of these specimens are not inconsistent with MDAC; sediments with a similar description, sampled from inter-tidal deposits on the Firth of Forth by the author, have $^{13}\delta C$

signature of MDAC (unpublished data). These areas, and much of the seabed south and east of the isle of Arran are underlain by potential source rocks of Carboniferous (Westphalian) age (Fig. 2b), so it is quite possible that these specimens are composed of MDAC, and that MDAC occurs elsewhere in the Firth.

3.8 Conclusions

The presence of MDAC has been confirmed at two sites: Texel 11 and Holden's Reefs. At other sites, although not confirmed, the possibility that MDAC is present is suggested by the presence of one or more of the following indicators: potential methane sources, gas migration pathways, shallow gas, elevated methane concentrations in sediment porewaters, elevated methane concentrations in seawater, and pockmarks. The distribution of potential sources of methane of Holocene to Carboniferous ages, and the availability of fluid migration pathways, suggest that there is potential for MDAC formation at sites and in areas covered neither by existing publications, nor by the SEA6 surveys.

Substantial seabed cliffs have been reported at Pisces Reef (a rocky reef). The less substantial cliffs at Harvey Trench, Texel 10, and Texel 11 are impressive in that they formed by the erosion of relatively soft clays of late-Pleistocene age.

4 THE LIKELY DISTRIBUTION AND EXTENT OF METHANE-DERIVED AUTHIGENIC CARBONATE

As a result of the investigations described in Section 3 it is concluded that gas in seabed sediments, its escape to the water column, and the formation of features associated with MDAC, as well as confirmed occurrences of MDAC formation, are associated with methane sources of various ages (Carboniferous, Oligocene-Miocene, and Holocene). Sources of other ages present elsewhere in the SEA6 area have similar potential to 'feed' MDAC formation. Of the two sites at which MDAC has been identified one (Texel 11) is associated with a sub-cropping source, the other (Holden's Reefs) with the fault-bounded edge of a basin. Of all the sites surveyed, those in which evidence of shallow gas and other indicators of MDAC all were similarly associated with potential sources and migration pathways.

The distribution of MDAC in the SEA6 is estimated by assessing 'risk'. For the risk analysis illustrated in Fig. 97 (overleaf) it is assumed that areas with no potential source have a minimal likelihood of MDAC being present; a low risk. Risk increases where there is a potential source, and increases again where there is a viable migration pathway. So, areas coloured dark grey on Fig. 97 (underlain by a pre-Holocene source) have a low risk, except where this source sub-crop beneath the Quaternary sediments (light yellow areas), or where faults or salt structures (orange) may provide a migration pathway; in these places risk is considered to be high. Experience from the Peel Basin II and Yuan's Pockmarks areas suggests that risk in areas with a Holocene source (light grey) is also dependent upon the nature of the sea sediment. It might be assumed that areas with very shallow gas, high methane concentrations, pockmarks, and documented evidence of gas seepage; however, no evidence of MDAC was seen in the active pockmarks surveyed. In contrast, MDAC has been documented in active pockmarks in the North Sea, where the seabed sediments are somewhat stiffer. It is therefore speculated that MDAC risk decreases in very soft sediments, even where other indicators are present. MDAC may therefore be more likely to occur in Lune Deep, for example.

The extent of MDAC in areas where it is present is more difficult to predict. Generally, it might be assumed that MDAC will be restricted to specific locations where migration pathways are present; for example, in the vicinity of faults. This assumption is consistent with MDAC occurrences found in association with faults, mud volcanoes etc. in other areas where MDAC, sulphidic sediments, *Beggiatoa* mats and cold seep communities are very localised (generally <100 m in extent, and often patchy even within such small areas). This model probably explains the Holden's Reefs occurrence; the proximity of Holden's Reefs to the Mochras Fault at the edge of the Cardigan Bay Basin supports speculation that the reef is fuelled by gas derived from Oligocene-Miocene lignites, the fault zone aiding vertical migration. If this is the case, then more, localised, occurrences of MDAC might be found at comparable locations along this and other faults bounding the basin, and in comparable locations elsewhere. For example, individual faults associated with St George's Wall might permit migration, leading to localised MDAC formation at the seabed.

The more widespread extent of MDAC at Texel 11 suggests less localised gas migration; in this case coarse layers within the Prograded Facies are thought to enable migration, MDAC formation occurring where these layers outcrop at the seabed. Further occurrences of widespread MDAC might therefore be expected wherever the Prograded Facies, or similar sediments, overlies a viable source, and outcrops at the seabed, for example in Central Trench and Texel 10. [Although no MDAC was recovered from the Prograded Facies cliffs at Texel 10, further sampling may prove that it is present.]

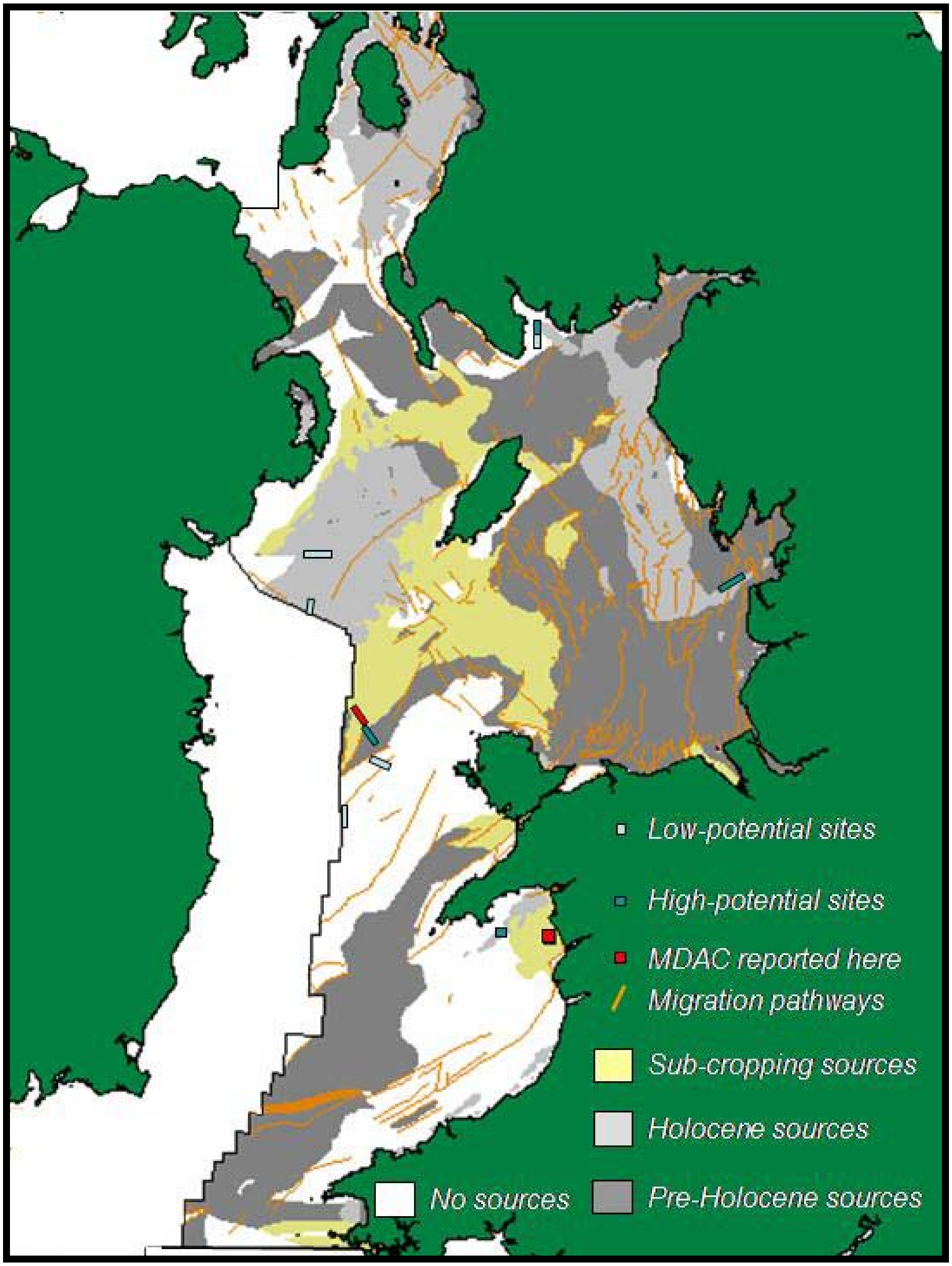

Figure 97: MDAC risk map: the likelihood of MDAC occurrences is highest in areas underlain by a methane source, and where either the source sub-crops beneath the Quaternary cover, or where faults provide a migration pathway.

5 THE SIGNIFICANCE OF THE TEXEL REEFS AND HOLDEN'S REEF

The Texel Reefs and Holden's Reefs are unlike other occurrences of MDAC described to date in UK waters. Other known occurrences are:

- Occurrences in the Witch Ground Basin of the North Sea are restricted to the bases of active pockmarks. Judd (2001) described three occurrences in UK block 15/25), but unpublished evidence of other occurrences has been brought to light by the petroleum industry.
- Carbonate hard-grounds on the foreshore at Society on the southern shore of the Firth of Forth (described by Andrews, 1988) have been confirmed as MDAC by carbon isotope analysis ($\delta^{13}C$ = -44.65‰$_{PDB}$; A.G. Judd, unpublished data).
- Scoffin (1988) reported "*one or two occurrences*" of localised hardgrounds to the west of Scotland; a sample from the Passage of Tiree was confirmed as MDAC ($\delta^{13}C$ -36.5‰).

Unconfirmed, but probable, occurrences of MDAC are:

- The description of a carbonate sample dredged from Fetlar Deep, Shetland Islands, is consistent with MDAC (Sabine and Wood, 1970); associated fauna described by Sabine and Wood included *Lucinoma borealis*, a bivalve hosting endosymbiotic sulphur oxidising microbes, described by Dando (2001) as present in the open North Sea only in association with methane seeps.
- Hard grounds occurring above the salt diapir of the Machar field (UK block 23/26; described by Salisbury, 1990 and Thrasher *et al.* 1996) are similar in appearance (on geophysical data) and geological context to the well-documented salt diapir-associated MDAC occurrences of the Tommeliten field in the Norwegian North Sea (Hovland and Judd, 1988). It is probable that MDAC also occurs above other salt diapirs in the North Sea (e.g. those of the Banff, Monan, Mungo, and Pierce fields).

None of these occurrences is as extensive as either Holden's Reefs (40,000 m^2) or the Texel Reefs (possibly >500,000 m^2); compared to these reefs, occurrences of MDAC in pockmarks seem to be particularly restricted.

6 OTHER ISSUES RAISED

The results discussed above raise a number of issues which lie beyond the scope of this study. These are principally concerned with processes related to the formation of the MDAC at Texel 11 and Holden's Reef, and to the formation of the trenches in the Central Irish Sea.

Substantial volumes of methane were required to form the masses of MDAC forming Holden's Reefs and the Texel Reefs, and the formation process involved microbial processing on an 'industrial' scale. This has the following potential implications:

- Apart from the benthic macrofauna attracted to the hard substrate (the MDAC), it is likely that there are benthic micro-, meio-, and macro-faunal communities associated with the anaerobic methane oxidation which has resulted in MDAC formation.
- Considerable quantities of methane may have passed into the water column; much of this will have been oxidised. As methane oxidation is microbially mediated, there are implications for the marine ecology.
- Substantial methane fluxes into the water column may result in significant fluxes of methane (an important greenhouse gas) into the atmosphere, whether by the escape of bubbles, or by a sea:air flux driven by differential methane concentrations.

The juxtaposition of MDAC and elevated methane concentrations with seabed hollows (in Texel 11) and trenches (as at Jürgen's Nightmare, Harvey Trench) suggests that gas escape may have been involved in seabed erosion and the formation of these features. Were this to be the case, gas escape would have to be recognised as a potent mechanism for erosion with the potential to generate features far larger than the pockmarks of the Western Mud Belt and other areas such as the North Sea.

6.1 Suggestions for further work

1. Sites identified as possible MDAC sites identified in this report (Lune Deep, Wigtown Bay, Yuan's Pockmarks, and St George's Wall) require further investigation, as do sites in the Firth of Clyde from which there have been reports of carbonate (?MDAC).

2. The MDAC occurrences of Texel 11 and Holden's Reef are worthy of more detailed investigation. Specifically this work should:
   - <u>Establish the true extent of the reefs</u>. In the case of Holden's Reef the work undertaken for SEA6 has established the extent of the reefs in the vicinity of the original discovery reef; however, additional reefs might be associated with other faults bounding the Tertiary basin in Tremadog Bay. The Texel 11 reefs clearly extend beyond the SEA6 survey area; it is possible that more detailed photography and sampling of the cliffs in Texel 10 and Harvey's Trench might also prove the presence of MDAC. Establishing the extent of the reefs would shed light on methane sources and geological controls to migration; this would facilitate searches for reefs in other areas, and other questions addressed below.
   - <u>Investigate the ecology of the reefs</u>. This work should include not only the macrofauna colonising the MDAC, but also the micro-, meio-, and macro-benthic infauna so that the rate and significance of methane utilisation can be ascertained.
   - <u>Determine the source of the methane</u>. Although Tertiary and Carboniferous ages have been suggested for Holden's Reef and the central Irish Sea area respectively, gas sampling, and carbon and hydrogen isotope analyses combined with detailed gas chromatography are required to confirm this. Without a

confirmation of the source discussions about the true extent of the reefs will contain an element of conjecture.

- Establish the time period over which the MDAC was formed, and the methane flux. Clearly, both the Texel 11 and Holden's Reef MDAC occurrences represent formation over an extended time period. Quantifying this time period will enable average methane flux rates to be determined; this would shed light on the role of this geological methane on:
    - benthic and water column ecology;
    - seabed processes, particularly the possible role of gas escapes in the seabed erosion and the formation of the hollows and trenches in the central Irish Sea;
    - contributions to atmospheric methane concentrations today and in the past.

3. The MDAC occurrences identified in the Irish Sea during this SEA6 project confirm that MDAC is not confined to pockmarks. A re-evaluation of the likely distribution and extent of MDAC in UK waters is therefore called for.

REFERENCES

Abril, G. and Iversen, N., 2002, Methane dynamics in a shallow non-tidal estuary (Randers Fjord, Denmark). *Marine Ecology-Progress Series*, **230**, 171-181.

Al-Shaikh, Z.D., 1970. *Geophysical Investigations in the Northern Part of Cardigan Bay (Including Part of the Central Irish Sea).* Unpublished PhD thesis, Aberystwyth.

Andrews, J.E., 1988. Methane-related Mg-calcite cements in recent tidal flat sediments from the Firth of Forth. *Scottish Journal of Geology*, 24, 233-244.

Caston, V.N.D., 1966. *A Study of the Recent Sediments and Sedimentation in Tremadog Bay, North Wales.* Unpublished PhD thesis, Aberystwyth.

Coplen, T.B., Kendall, C. and Hopple, J., 1983. Comparison of stable isotope reference samples. *Nature*, **302**, 236-238.

Croker, P.F., 1994. Shallow Gas in the Irish Sea and Associated Seafloor Morphology, *3rd Conference on Gas in Marine Sediments*, Texel, The Netherlands, Shallow Gas Group (Poster).

Croker, P.F., 1995. Shallow Gas Accumulation and Migration in the Western Irish Sea, IN: Croker, P.F. and Shannon, P.M. (ed.), *The Petroleum Geology of Ireland's Offshore Basins*, Geological Society of London, London, Special Publication 93, 41 - 58.

Croker, P.F., 1998. *Report of the Celtic Voyager cruise of April 1998.* Internal report, Petroleum Affairs Division, DCMNR, Dublin, Ireland (unpublished).

Croker, P., Garcia-Gil, S. and Monteys, X., 2002. A Multibeam Survey of the Codling Fault Zone, Western Irish Sea, *Gas in Marine Sediments* conference, Baku, Azerbaijan.

Croker, P.F., Monteys, X. and O'Loughlin, O., 2002. A Multibeam Survey of the Codling Fault Zone, 2001-2002, *Marine Geophysical Investigations in Ireland today*, GAI / GSI / PESGB, Presentation.

Dando, P.R., 2001. *A review of pockmarks in the UK part of the North Sea, with particular respect to their biology.* TR_002, Department of Trade and Industry, 21p.

EC, 1997. Council Directive 97/62/EC of 27 October 1997 Adapting to Technical and Scientific Progress Directive 92/43/EEC on the Conservation of Natural Habitats and of Wild Fauna and Flora. *Official Journal*, **L305**, 42-65.

EC, 1999. *Interpretation Manual of European Union Habitats.* European Commission (DG Envrionment), 121p.

Eden, R.A., Deegan, C.E., Rhys, G.H., Wright, J.E. and Dobson, M.R., 1973. *Geological investigations with a manned submersible in the Irish Sea and off western Scotland, 1971.* Report 73/2, Institute of Geological Sciences, HMSO, London, 8p.

EEC, 1992. Council Directive 92/43/EEC of 21 May 1992 on the Conservation of Natural Habitats and of Wild Fauna and Flora. *Official Journal*, **L206**, 7-50.

Evans, D., 1985. *Clyde Sheet 55N-06W Seabed Sediments & Quaternary.* 1:250,000 Map Series, British Geological Survey.

Farrow, G.E., 1983. Recent Sediments and Sedimentation in the Inner Hebrides. *Proceedings of the Royal Society of Edinburgh*, **83B**, 91 - 105.

Garrard, R.A., 1977. The Sediments of the South Irish Sea and Nymphe Bank Area of the Celtic Sea., IN: Tooley, M.J. (ed.), *The Quaternary History of the Irish Sea*, Geological Journal Special Issue No. 7, Liverpool, 69-92.

Harvey, J.G., 1966. Large sand waves in the Irish Sea. *Marine Geology*, 4, 49-55.

Hession, M.A. and Whittington, R.T.R., 1987. Aspects of the Quaternary Sediments of the Anglesey Sheet. *Proceedings of the Geologists' Association*, **98**, 398-400.

Hession, M.A.I., 1988. *Quaternary Geology of the Southern Irish Sea*. Unpublished thesis, University of Aberystwyth.

Hovland M. and Judd, A.G., 1988. *Seabed Pockmarks and Seepages, Impact on Geology.* Graham and Judd, A.G. Trotman Ltd, London, 293 pp.

Jackson, D.I., Jackson, A.A., Evans, D., Wingfield, R.T.R., Barnes, R.P. and Arthur, M.J., 1995. *The Geology of the Irish Sea*. BGS UK Offshore Regional Report HMSO, London, 123p.

James, J.W.C. and Wingfield, R.T.R., 1988. *Cardigan Bay Sheet 52n-06w Including Part of Waterford 52N-08W and Mid-Wales & Marches 52n-04w. Seabed Sediments.* 1:250,000 Series, British Geological Survey.

James, J.W.C. and Wingfield, R.T.R., 1990. *Anglesey 53N 06W: Sea Bed Sediments*: 1:250,000 Map Series, British Geological Survey.

Johnston, C.M., Turnbull, C.G. and Tasker, M.L., 2002. *Natura 2000 in UK Offshore Waters: Advice to Support the Implementation of the EC Habitats and Birds Directives in Uk Offshore Waters.* JNCC Report 325, Joint Nature Conservation Committee, 155p.

Jones, G.B., Floodgate, G.D. and Bennell, J.D., 1986. Chemical and Microbiological Aspects of Acoustically Turbid Sediments: Preliminary Investigations. *Marine Geotechnology*, **6**, 315 - 332.

Judd, A.G., 2001. *Pockmarks in the UK Sector of the North Sea.* TR_002, Department of Trade and Industry, 73p.

Osiris Projects Ltd., 2005. *Irish Sea – Inshore Sector*. Geophysical Report. SEA6.

Pantin, H.M., 1977. Quaternary Sediments of the Northern Irish Sea, IN: Kidson, C. (ed.), *The Quaternary History of the Irish Sea*, Geological Journal Special Issue No. 7, 27 - 54.

Pelagial Ltd., 2005. *Across-Wales diving monitoring project.* Interim Report for Cynor Cefu Gwlad Cymru / Countryside Council for Wales; Contract No. FC 73-020292 (unpublished).

Sabine, P.A. and Wood, C.J., 1970. A bowl-like object of aragonite-limestone from Shetland waters. *Proceedings of the Geological Association* 81, 539 - 548.

Salisbury, R.S.K., 1990. Shallow gas reservoirs and migration paths over a Central North Sea diapir. In, Ardus, D.A. and Green C.D. (Eds.) *Safety in Offshore Drilling: the role of shallow gas surveys.* Kluwer Academic Publishers, Dordrecht, 167-180.

Scoffin, T.P., 1988. The environments of production and deposition of calcareous sediments on the shelf west of Scortland. *Sedimentary Geology*, 60, 107-124.

Tappin, D.R., 2004. *SEA6 Survey Preparation - Sedimentary Processes and Survey Scoping Study.* CR/04/142, British Geological Survey, 32p.

Tappin, D.R., Chadwick, R.A., Jackson, A.A., Wingfield, R.T.R. and Smith, R.T.R., 1994. *The Geology of Cardigan Bay and the Bristol Channel*. British Geological Survey, London, 107p.

Taylor Smith, D., 1987. Geotechnical Studies in Tremadog Bay. *Proceedings of the Geologists' Association*, **98**, 385 - 396.

Thrasher, J., Fleet, A.J., Hay, S., Hovland, M. and Düppenbecker, S., 1996. Understanding geology as the key to using seepage in exploration: The spectrum of seepage styles. In: Schumacher, D. and Abrams, M.A. (eds) *Hydrocarbon migration and its near-surface expression.* American Association of Petroleum Geologists, Memoir 66, 223-241.

Upstill-Goddard, R. C., Rees, A. P. and Owens, N. J. P., 1996, Simultaneous high-precision measurements of methane and nitrous oxide in water and seawater by single phase equilibration gas chromatography. *Deep-Sea Research I*, **43**, 1669-1682.

Vincent, M.A., Atkins, S.M., Lumb, C.M., Golding, M., Lieberknecht, L.M. and Webster, M. 2004. *Marine nature conservation and sustainable development – the Irish Sea Pilot.* Report to Defra by the Joint Nature Conservation Committee, Peterborough.

Wingfield, R.T.R., 1983. *Lake District 54N 04W: Sea Bed Sediments and Quaternary Geology*: 1:250,000 Map Series, British Geological Survey.

Wingfield, R.T.R., 1984. *Liverpool Bay 53N 04W: Sea Bed Sediments and Quaternary Geology*. 1:250,000 Map Series, British Geological Survey.

Wingfield, R.T.R., 1985. *Isle of Man 54N 06W: Seabed Sediments and Quaternary Geology*. 1:250,000 Map Series.

Wingfield, R.T.R., 1990. *Anglesey 53N 06W: Quaternary Geology.* 1:250,000 Map Series, British Geological Survey.

Wingfield, R.T.R., Hession, M.A.I. and Whittington, R.T.R., 1990. *Cardigan Bay 52n - 06w: Quaternary Geology*. 1:250,000 Map Series,

Yuan, F., 1994. *Acoustic and Geotechnical Properties of the Western Irish Sea Sediments.* Unpublished PhD thesis, Bangor.

Yuan, F., Bennell, J.D. and Davis, A.M., 1992. Acoustic and Physical Characteristics of Gassy Sediments in the Western Irish Sea. *Continental Shelf Research*, **12**, 1124 - 1134.

Acknowledgements

The following are acknowledged for their contributions to the project summarised in this report: Peter Croker (PAD, Dublin) provided a wealth of data and ideas, and commented on the manuscript; the captains and crews of S/V *Meridian* and S/V *Kommandor Jack*; personnel from OSAE, survey and geophysical contractors on the *Meridian*, and survey contractors on the *Kommandor Jack*; Louise Tizzard provided GIS support throughout the project; personnel from Seastar and ERT undertook the photographic surveys and sampling on the *Kommandor Jack*; colleagues in the Ocean Research Group, University of Newcastle-upon-Tyne provided analytical services; Carolyn Voisey and personnel from Osiris Projects undertook the surveys on S/V *Lia*; Rohan Holt (CCW) provided photographs and a sample of Holden's Reefs; Dave Tappin and colleagues at BGS provided useful discussions. This project was managed by Quentin Huggett and Sally Marine of Geotek, who provided invaluable support during the survey operations. Paul Dando critically reviewed the manuscript.

Appendix I

Survey Equipment Details

SEA6 Surveys, 2004

Geophysical Surveys – S/V *Meridian*

[Equipment operated by OSAE]

Surface positioning:

Trimble 4000 Differential GPS.

Underwater positioning:

Nautronix ATS II USBL.

Multi-beam echo sounder (MBES):

Reson 8101 multibeam echo sounder: 240 kHz, 150º swathe, 1.5º x 1.5º, 100 beams linked to iXSea Octans laser gyro/motion reference unit.

Single Beam Echosounder (SBES):

Atlas Deso 25 hydrographic echo sounder operating at 210 or 33 kHz.

Side-scan sonar (SSS):

Edgetech DF 1000 digital side-scan sonar: linked to Triton Elics digital data acquisition / sonar enhancement system.

Sub-bottom profiling (SBP):

Benthos Chirp II profiler: operating at 2-7 or 8-23 kHz, vessel-mounted transducer array, 4kW output.

Sound velocity / CTD:

AMS Smart Probe.

Data systems:

Navigation and MBES acquisition: QPS Qinsy
MBES processing: CARIS / HIPS / HDCS
SSS processing: SIPS modules of CARIS / HIPS
SBP editing and enhancement: Benthos CAP 6600
SBP further processing: Sandmeier Reflex
Charting: AutoCad with AutoChart.

Photographic surveys and sampling
S/V *Kommandor Jack*

[contractors are identified in brackets]

Surface positioning [OSAE]:

Trimble 4000 Differential GPS.

Underwater positioning [OSAE]:

Nautronix ATS II USBL.

Sound velocity / CTD [OSAE]:

AMS Smart Probe.

Data systems [OSAE / L. Tizzard]:

Navigation: Navipak
Positioning data were then converted, using bespoke OSAE software, to formats suitable for GIS (ArcView / ArcExplorer) applications.
ArcView 3.1 was then used to create .shp files for ArcExplorer use (decision making and interpretation).

Photography [SeaStar]:

OE14-108 Kongberg Simrad underwater digital stills camera mounted on a stainless steel frame, with 3 24-volt lamps, and a flash unit, powered from a 360 to 24 volt transformer. Image capture and storage computer-operated using a 14-108GUI graphic user interface, enables both digital and analogue video capture, and digital still capture.

ROV [SeaStar]:

Seabotix LBV150 remotely operated vehicle, providing digital video output (recorded using SeaStar digital and analogue video recorders).

Sampling [ERT]:

Day grab
NIO water bottles

Appendix II

Methane concentrations in sediment porewaters

Analyses performed by

Ocean Research Group
School of Marine Science & Technology
University of Newcastle upon Tyne

Area	Station	Sample Number	Temperature ºC	Salinity ‰	CH_4 nmol.l^{-l}	CH_4 saturation %
Yuan's Pockmarks	YMP2_station1	2	13.49	34.1	150	6,210
	YMP4_station2	2	13.49	34.1	190	7,945
	YMP1_station1	2	13.49	34.1	230	9,495
	YMP1_station2	4	13.49	34.1	25	960
	YMP1_station4	2	13.49	34.1	25	965
	YMP1_station3	2	13.49	34.1	4,230	177,230
	YMP3_station1	2	13.49	34.1	1,090	4,530
	YMP3_station2	2	13.49	34.1	4,710	197,210
	YMP3_station3	3	13.49	34.1	70	2,870
	YPM5_station1	3	13.49	34.1	65	2,645
Harvey Trench	HT_station2	1	14.15	34.66	25,095	1,070,090
	HT_station1	3	14.15	34.66	60	2,615
	HT_station4	1	14.15	34.66	2,710	115,440
Texel 10	T10_station2	1	14	34.7	50	2,180
	T10_station3	1	14	34.7	120	5,165
	T10_station6	2	14	34.7	200	8,550
	T10_station7	4	14	34.7	180	7,750
	T10_station11	1	14	34.7	245	10,340
Tremadog Bay	TT0	0B	-	-	36,335	1,656,910
	TT1	1C	-	-	53,485	2,438,850
		1F	-	-	2,065	94,230
	TT2	2C	-	-	8,460	385,760
	TT3	3C	-	-	28,065	1,279,240
		3F	-	-	835	38,040
Muddy Hollow	MH4	4A	-	-	5,190	236,730
		4B	-	-	5,855	267,000
Holden's Reef	HRG1	1C	-	-	560	25,550
	HRG2	2C	-	-	5,796,800	264,331,170
		2F	-	-	51,210	2,334,990
	HRG3	3D	-	-	33,780	1,540,400
		3E	-	-	3,560	162,190
	HRG4	4D	-	-	133,830	6,102,650
		4E	-	-	48,400	2,207,100
	HRG5	5A	-	-	9,465	431,530

Differences between methane concentrations in samples taken from sites close together (e.g. TT1C and TT1F) indicate extreme variability caused by the geological focussing of seabed fluid flow.

Appendix III

Carbon isotope analyses of carbonate samples

Analyses performed by

Iso-Analytical Ltd.

Iso-Analytical Laboratory Report

Client Details

Client:	Dr. Alan Judd

Sample Details

Number:	10
Material:	Seabed sediments

Sample Tracking

IA Reference No.:	041123-1
Date of Arrival:	23/11/2004 (9) 30/11/2004 (1)

Analysis Details

Isotope(s) :	Carbon-13 and Oxygen-18
Method:	CF-IRMS
Report Date:	15/12/2004

Duplicate results shown in **BOLD**

Sample Identification	*Amount of sample used (mg)	Result $\delta\text{-}^{13}C_{V\text{-}PDB}$	Mean $\delta\text{-}^{13}C_{V\text{-}PDB}$
Society MDAC	9	-44.65	
Marine carbonate	2	1.70	
T11/1/1	**6**	**-43.06**	
"	**6**	**-41.84**	**-42.45**
T11/4/1	6	-41.16	
T11/6/1	18	-17.55	
T11/9/2	**7**	**-46.17**	
"	**7**	**-46.56**	**-46.36**
T11/10/4	9	-26.70	
T11/11/1	7	-46.43	
T11/12/2	8	-34.64	
HR/CCW/1	**7**	**-33.81**	
"	**7**	**-33.98**	**-33.90**

*Measured against a reference of 2 mg pure calcium carbonate

Quality Control-Reference Standards

Reference Standard	Reference Material	$\delta\text{-}^{13}C_{V\text{-}PDB}$ (‰)	Mean $\delta\text{-}^{13}C_{V\text{-}PDB}$ (‰)
NBS-18	Calcite	-5.04	
"	"	-5.04	-5.04
		accepted=	-5.00
NBS-19	Limestone	1.88	
"	"	1.93	1.91
		accepted=	1.95
IAEA-CO-8	Carbonatite	-5.76	
"	"	-5.80	-5.78
		accepted=	-5.80
IA-R022	Calcium Carbonate	-28.73	
"	"	-28.63	
"	"	-28.62	-28.66
		accepted=	-28.63

Appendix IV

Methane concentrations in seawater samples

Analyses performed by

Ocean Research Group
School of Marine Science & Technology
University of Newcastle upon Tyne

SEA6 Date	Depth (m)	Water Depth (m)	Lat	Long	Underway Station Number	Methane in situ nmol / l	Methane Saturat'n Percent
29/11/2004	2	118	53.114738	-5.308991	CE_2_water1	2.82	119.9
29/11/2004	2	118	53.114241	-5.309135	CE_2_water2	2.90	123.2
29/11/2004	2	85	53.417687	-5.198473	T10_water1	3.51	149.8
29/11/2004	43	85	53.417687	-5.19846	T10_water2	2.83	120.7
29/11/2004	80	85	53.417735	-5.198433	T10_water3	2.99	127.5
29/11/2004	2	95	53.414646	-5.19142	T10_water4	2.80	119.4
29/11/2004	47	95	53.414731	-5.191423	T10_water5	3.77	161.2
29/11/2004	92	95	53.414738	-5.191428	T10_water6	2.72	116.3
29/11/2004	2	85	53.417694	-5.198276	T10_water7	2.94	125.6
29/11/2004	42	85	53.417718	-5.198318	T10_water8	2.80	119.6
29/11/2004	82	85	53.417648	-5.19841	T10_water9	2.41	103.1
29/11/2004	2	100	53.408322	-5.182893	T10_water10	2.96	126.5
29/11/2004	47	100	53.408343	-5.182868	T10_water11	2.94	125.5
29/11/2004	94	100	53.408335	-5.182793	T10_water12	2.68	114.5
29/11/2004	2	100	54.000599	-5.502558	YPM5_station 2	10.64	447.5
29/11/2004	95	100	54.000636	-5.50233	YPM5_station 2	6.73	283.0
29/11/2004	50	100	54.000692	-5.502382	YPM5_station 2	8.17	343.7
29/11/2004	110	110	53.996657	-5.484571	YPM1_station 4	32.74	1377.2
29/11/2004	56	110	53.996726	-5.48452	YPM1_station 4	5.95	250.3
29/11/2004	2	110	53.996726	-5.484506	YPM1_station 4	21.03	884.0
29/11/2004	5	190	53.308486	-5.094921	HT_3_water1	2.53	108.3
29/11/2004	90	190	53.307663	-5.09502	HT_3_water1	2.63	112.5
29/11/2004	172	190	53.30881	-5.094956	HT_3_water1	3.10	132.6